Qeios

Research Article

Auditory Tract Maturation in Early Infancy: Links to Speech Production

飞鸿刘[1], Yaoxuan Wang[2,3,4], Jinchen Gu[5], Jiameng Liu[5], Xinyi Cai[5], Han Zhang[6], Jun Feng[1], Zhaoyan Wang[2,3,4], Hao Wu[2,3,4], Dinggang Shen[6,7]

1. School of Information and Technology, Northwest University, China; 2. Department of Otolaryngology-Head and Neck Surgery, Shanghai Jiao Tong University, Shanghai, China; 3. Ear Institute, China; 4. Shanghai Key Laboratory of Translational Medicine on Ear and Nose Diseases, China; 5. School of Biomedical Engineering & State Key Laboratory of Advanced Medical Materials and Devices, ShanghaiTech University, Shanghai, China; 6. Shanghai Clinical Research and Trial Center, China; 7. Shanghai United Imaging Intelligence Co., Ltd., China

Infants exhibit remarkable language acquisition abilities, supported by highly plastic neural substrates that dynamically interact with early speech experiences. However, the developmental mechanisms of these neural substrates and their specific role in speech acquisition remain incompletely understood. Here, we present NeoAudi Tract (NAT), a robust automated toolbox for extracting the full set of auditory tracts in infants from birth to 24 months using 3T diffusion MRI data. By characterizing the microstructural changes in these tracts, we demonstrate a gradual and continuous maturation process of the auditory system. Additionally, we identify significant correlations between auditory tract maturation and both *fine-motor skills* and *expressive language t-scores* from the Mullen Scales of Early Learning tests. Our findings highlight the role of the auditory system in speech production and indicate the intertwined development of auditory and motor systems that underlies speech acquisition, particularly during perceptual reorganization.

Corresponding authors: Jun Feng, fengjun@nwu.edu.cn; Zhaoyan Wang, napoleon1982@gmail.com; Hao Wu, wuhao@shsmu.edu.cn; Dinggang Shen, Dinggang.Shen@gmail.com

1. Introduction

Infants are unparalleled language learners, endowed with highly plastic neural substrates that rapidly adapt to early speech experiences, enabling the swift acquisition of essential communicative and cognitive skills[1][2][3]. On the one hand, ongoing neural development progressively enhances the ability to detect and recognize speech patterns, from basic linguistic structures to complex, high-level ones[4][5]; on the other hand, these speech experiences shape the maturation of the underlying neural circuits[6]. A hallmark of speech acquisition during this period is the shift from a universal sensitivity to phonetic contrasts across all languages in early infancy, to a more specialized sensitivity attuned to the language(s) infants regularly hear by the end of the first year. This transformation is commonly referred to as *perceptual reorganization*, *perceptual attunement*, or *perceptual narrowing*[7][8][9][10]. Crucially, the maturation of the relevant neural substrates in this period not only facilitates communicative speech abilities[11], but

also lays a foundation for broader intellectual skills, including reading, mathematics, and general cognitive ability (*e.g.*, IQ) in later childhood[12][13][14][15][16]. Despite this growing body of evidence, the precise mechanisms by which these neural substrates develop to support perceptual reorganization for speech remain poorly understood. Clarifying how early speech experience interacts with the neural circuits may therefore be pivotal for advancing our understanding of both language development and broader cognitive outcomes.

Recent research indicates that speech processing relies on the functional integration of the auditory and motor systems[17][18][19][20]. While auditory and motor processing predominantly contribute to speech perception and production, respectively[21][22][23][24], they also interact in each other's processing[18][25]. The auditory system, for instance, may engage in motor learning[26], thereby influencing speech production[27]. However, these mechanisms remain less understood than the motor system's role in speech perception[28].

Numerous studies have demonstrated the critical role of the motor system in speech perception[29][30][31][32][33][34], showing that speech perception is an active process rather than a passive process[35][36]. Notably, the motor system compensates for speech perception in noisy or distorted cases by enhancing the activities of components in the motor system[37][38]. Direct stimulation of articulatory regions in the motor cortex specifically interferes with the recognition of corresponding phonemes[18][39][40], and restricting articulatory movements of the lips or tongue similarly disrupts phoneme identification[41][42][43][44]. Taken together, these findings underscore the critical importance of linking aural (speech perception) and oral (speech production) processes[45]. Although associations between auditory and motor systems have been observed in infants[46], as young as 3 months of age[47], *they may not be present at birth*[48]. Consequently, current research increasingly focuses on early-life sensorimotor experiences that facilitate the establishment of these sensory-motor associations[49][50][51][52], rather than on isolated sensory or motor experiences[19][53][54][55].

Early-life experiences drive plastic changes in neural substrates, particularly in white matter, thereby enabling efficient transmission and synchronization of neural firing across functionally segregated brain regions[6][56][57]. The formation of a mature, interconnected brain network serves as the basis for a range of cognitive functions, including speech[58][59]. Thus, understanding the dynamics of white matter maturation can provide critical insights into the neural mechanisms underlying speech acquisition and cognitive development[60][61]. However, despite increasing evidence on the importance of white matter maturation, the specific contributions of auditory tracts to speech production, especially in the context of perceptual reorganization, remain unclear, underscoring the need for further investigation.

To non-invasively investigate the development of the white matter tracts in infants, diffusion MRI (dMRI) has emerged as the primary and widely employed technique[62][63][64][65][66][67]. Yet, extracting auditory tracts in infants poses unique challenges, due to their smaller size, complex structures, and considerable spatiotemporal variability of developing tissues[68][69].

Early investigations into auditory tract development have relied predominantly on histological observations, which provide a rough developmental timeline[70][71][72]. With subsequent advances in neuroimaging, these anatomical insights have been significantly enriched through non-invasive characterization of the tiny and complex auditory nuclei[73][74]. Given the minute size and complex structures of these brainstem nuclei and tracts, high-resolution imaging is required. Recent methodologies in adults have employed either *ex vivo* 3T MRI[75] or *in vivo* imaging with 7T scanners[74][76]. For infants, additional challenges arise. Shorter scanning times are required to accommodate unsettled conditions, which results in lower data quality[77]. Moreover, smaller brain sizes combined with spatiotemporal asynchrony lead to high variability in data distribution, complicating data acquisition, processing, and analysis[69][78]. Although BabyAFQ leverages the infant atlas developed in our prior studies[79] and a classical registration framework to extract 24 major tracts[78], it remains incapable of extracting auditory tracts. To address this gap, we constructed an auditory tract atlas by combining tract density imaging (TDI) with structural MRI (sMRI) data[68]. Despite these advancements, tools for extracting auditory tracts in infants remain scarce, highlighting the continued need for developing more specialized, automated approaches.

In this study, we propose an automated toolbox, *NeoAudi Tract* (NAT), for extracting the full set of auditory tracts spanning peripheral, subcortical, and cortical regions in infants from birth to 24 months. Leveraging 3T MRI data from the most comprehensive longitudinal Baby Connectome Project (BCP) dataset[80], we characterize the developmental trajectories of these auditory tracts, revealing a gradual and continuous maturation process. Auditory tracts closer to peripheral regions exhibit higher maturity, while those nearer to cortical regions show lower maturity. Notably, significant correlations were identified between auditory tract maturation and *fine-motor skills* and *expressive language t*-scores from the Mullen Scales of Early Learning (MSEL) tests, suggesting a potential influence of auditory processing on speech production. Furthermore, our results indicate that during early infancy, auditory tract development is intricately linked with the motor system, raising the possibility that the auditory system may, via motor mediation, play a role in attuning phonetic sensitivity during the first year of life. However, the precise maturation mechanisms through which the auditory system integrates with the motor system to subserve speech acquisition, particularly in the context of perceptual reorganization, remain unclear, highlighting the need for further investigation into the complex interplay between sensory and motor systems.

2. Results

Using our proposed NeoAudi Tract (NAT), we extracted the full set of auditory tracts from the longitudinal multi-shell high angular resolution diffusion imaging (HARDI) data in BCP[80] — one of the largest cohorts of infants with both high-quality neuroimaging data and behavioral scores assessed by the MSEL[81]. Our analysis focused on charting the developmental trajectories of these auditory tracts from birth to 24 months and examining their correlations with *t*-scores in four MSEL domains: *visual reception*, *fine-motor skills*, *receptive language*, and *expressive language*.

Of the entire dataset, 246 data samples (164 infants) passed the quality control (QC) procedures, as detailed in the Method section. Table 1 provides the sample sizes by age month. For correlation analysis, we selected MSEL t-scores from these data samples that were acquired within a 2-month window of their dMRI scanning time points, ensuring close temporal alignment. Fig. 1 illustrates the distribution of matched subjects across these intervals (122 infants, 189 data samples), including a subset older than 24 months to fully utilize the available longitudinal data.

Age	2 wk	1 mo	2 mo	3 mo	4 mo	5 mo	6 mo	7 mo	8 mo	9 mo	10 mo	11 mo	12 mo
Sample size (N)	5	2	1	9	9	17	14	10	14	17	7	13	17
Age		13 mo	14 mo	15 mo	16 mo	17 mo	18 mo	19 mo	20 mo	21 mo	22 mo	23 mo	24 mo
Sample size (N)		10	10	15	10	5	8	7	6	5	5	6	24

Table 1. Number of data samples per age month after quality control.
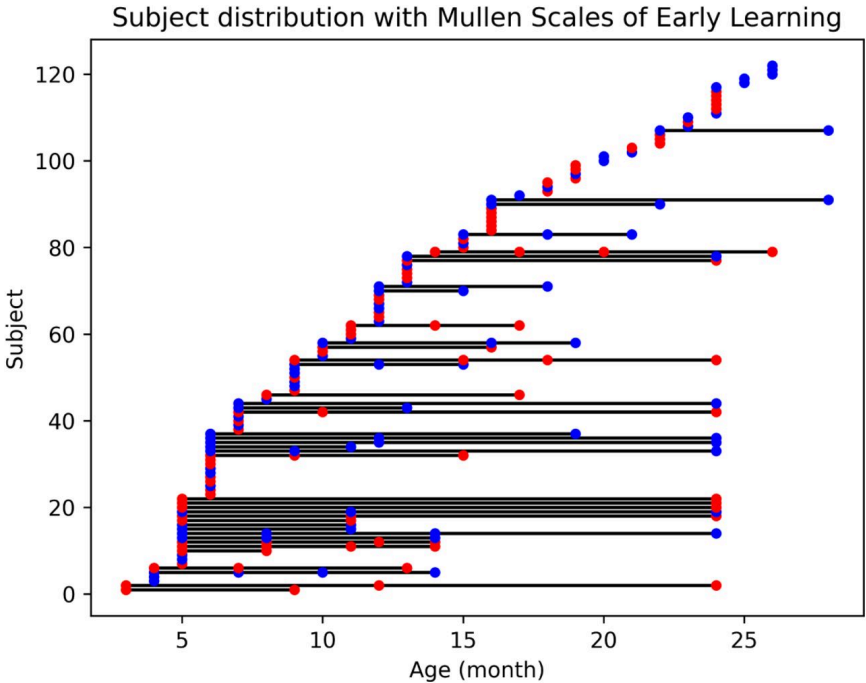

Figure 1. Distribution of subjects in the longitudinal study with paired MSEL scores and diffusion MRI data across different ages. The study includes data from 122 subjects (63 females and 59 males). Blue points represent males, red points represent females, and horizontal black lines connect data samples from the same individual.

2.1. Depiction of extracted auditory tracts

Fig. 2 illustrates the extracted auditory tracts and the aligned ROIs at six representative ages (3, 6, 9, 12, 18, and 24 months). These tracts and ROIs span peripheral, subcortical, and cortical regions[68][82]. More specifically, in the peripheral ear, the cochlea (CO) captures and converts speech vibrations into electrical pulses, which are transmitted via the cochlear nerve to the cochlear nucleus (CN). The signals then sequentially reach other brainstem and thalamic nuclei in the subcortical regions[82][83] before ultimately arriving at the primary auditory cortex (PAC) in the superior temporal cortex[84]. In total, we extracted 14 auditory tracts in this study, reflecting the comprehensive coverage of peripheral, subcortical, and cortical auditory pathways. As illustrated in Fig. 2, all auditory tracts were successfully identified, demonstrating the effectiveness of NAT for infant auditory tract extraction. From birth to 24 months, the streamlines of each tract become progressively denser, corresponding to the steady increase in brain size and myelination[69][85]. In younger infants (*e.g.*, 3 months), the extracted tracts appear noticeably smaller and sparser, reflecting the relatively underdeveloped brain structure at this early stage. By contrast, at 24 months, the tracts are visibly larger and denser, mirroring the ongoing maturation of white matter[86].
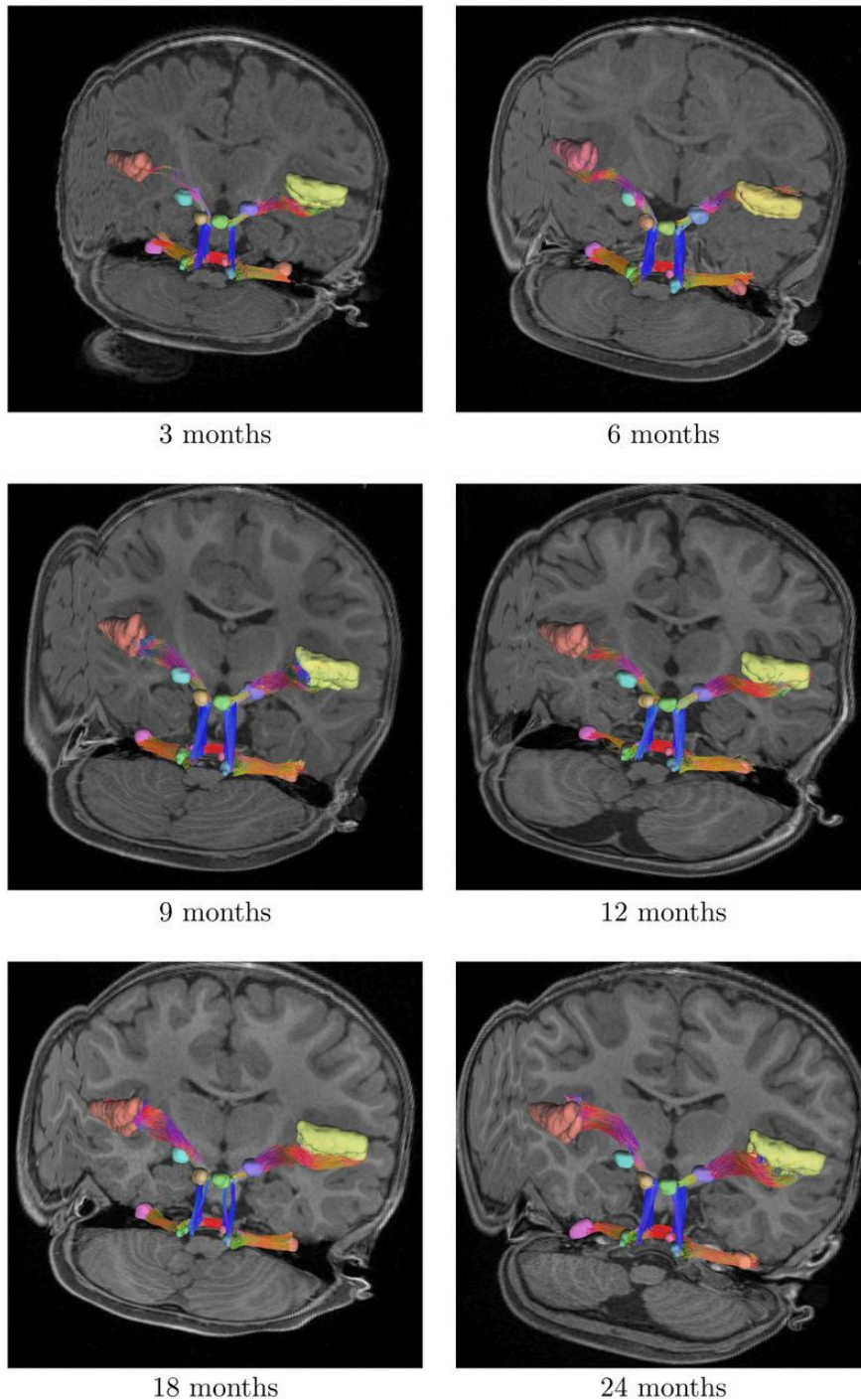
Figure 2. Extracted auditory tracts and aligned ROIs across six age periods (3, 6, 9, 12, 18, and 24 months). Tract size and streamline density increase progressively with age, reflecting ongoing brain development during early infancy.

To evaluate the effectiveness of NAT, we assessed the alignment of auditory nuclei — initial and terminal regions of these tracts — which determines the reliability of tract extraction. As illustrated in Fig. 3, we compared three

commonly used registration strategies for aligning adult templates with infant sMRI data:
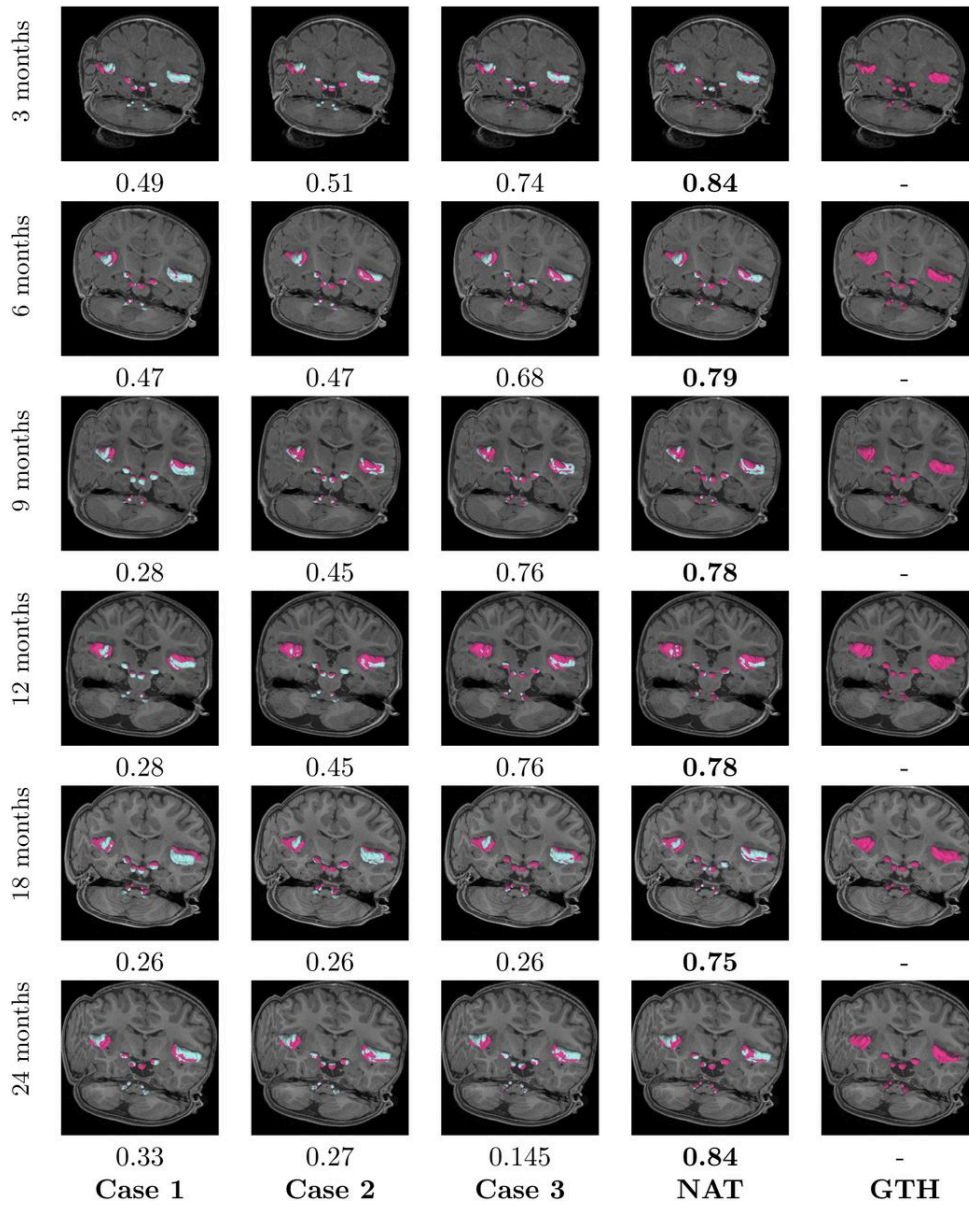

Figure 3. Alignment of auditory nuclei and averaged DICE scores () across four registration strategies: Case 1 – sMRI only; Case 2 – sMRI with tissue maps; Case 3 – sMRI with tissue maps and brainstem masks; and Case 4 – NAT. Incorporating tissue maps enhanced cortical alignment, while the inclusion of brainstem masks reduced errors in auditory nuclei alignment but introduced new alignment issues. The NAT achieved superior performance by separately aligning cortical and brainstem regions.

- **Case** 1: Registration using only sMRI data (T1w and T2w).
- **Case** 2: Registration using sMRI data combined with tissue maps to assist the alignment process.
- **Case** 3: Registration incorporating brainstem masks, in addition to tissue maps, to enhance brainstem alignment.

NAT builds upon a two-branch registration framework that separately aligns cortical and brainstem regions using sMRI data, tissue maps, and brainstem masks (see Fig. 10 in the Method section). As illustrated in Fig. 3, this approach outperforms Cases 1, 2, and 3, with NAT-aligned nuclei consistently exhibiting higher accuracy and closer correspondence to the ground truth (GTH) across all age periods. The GTH nuclei were manually labeled by a neuroradiologist with 15 years of expertise and subsequently reviewed by another with 29 years of experience, ensuring high accuracy and reliability. These findings underscore the robustness of NAT in aligning auditory nuclei under varying developmental periods.

2.2. Maturation of auditory tracts

To delineate the developmental trajectories of the auditory system, we characterized the maturation of auditory tracts and examined their correlations with MSEL t-scores in four domains: *visual reception*, *fine-motor skills*, *receptive language*, and *expressive language*. We assessed white matter microstructure using two complementary models: neurite orientation dispersion and density imaging (NODDI)[87] and diffusion tensor imaging (DTI)[88]. Specifically, these models were applied to generate microstructural attribute maps, including the neurite density index (NDI), radial diffusivity (RD), and fractional anisotropy (FA), thereby providing detailed information on white matter development throughout infancy.

We computed averaged NDI, RD, and FA values for each auditory tract, then modeled the population trajectories using a linear mixed effect model (LMM)[89]. As reported in Table 2, a quadratic model in the LMM provided superior performance, based on adjusted r-squared and Akaike information criterion (AIC), compared to the commonly used linear model. Although linear models are frequently employed to represent early white matter development[78][90], our results indicate that a quadratic model more accurately captures the non-linear trajectories of auditory tracts from birth to 24 months.

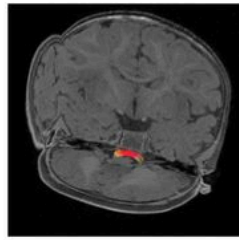|	CN$_L$-SOC$_L$	CN$_L$-SOC$_R$	CN$_R$-SOC$_R$	CN$_R$-SOC$_L$	CN$_L$-IC$_L$	SOC$_L$-IC$_L$	CN$_R$-IC$_R$	SOC$_R$-IC$_R$	BIC$_L$	AR$_L$	BIC$_R$	AR$_R$
Linear												
p	4.79e−26	1.89e−35	1.70e−26	3.05e−41	1.47e−27	1.69e−33	1.44e−33	6.43e−28	3.71e−41	6.47e−56	2.03e−41	1.48e−60
r^2 ↑	0.7140	0.8796	0.8074	0.8909	0.8818	0.7923	0.7408	0.7946	0.9068	0.8892	0.9011	0.8476
AIC ↓	−514.23	−816.07	−519.94	−836.21	**−716.33**	**−718.99**	**−694.47**	**−694.17**	−770.46	−874.04	−747.59	−871.90
Quadratic												
p	6.90e−17	2.00e−19	3.39e−12	3.65e−24	1.64e−09	6.97e−08	3.17e−12	9.87e−11	2.90e−25	3.28e−26	1.43e−16	7.84e−26
r^2 ↑	**0.8211**	**0.9319**	**0.8747**	**0.9032**	**0.9013**	**0.8110**	0.7675	**0.8038**	**0.9410**	**0.9254**	0.9055	**0.8950**
AIC ↓	**-524.66**	**-820.68**	**-528.20**	**-838.97**	-704.00	-698.70	-683.24	-690.49	**-793.89**	**-900.76**	**-750.89**	**-890.55**

Table 2. Comparison of linear and quadratic Linear Mixed-Effect Models for auditory tract NDI trajectories based on adjusted r-squared and AIC scores.

Abbreviations: AIC = akaike information criterion; L = left; R = right; CN = cochlear nucleus; SOC = superior olivary complex; IC = inferior colliculus; BIC = brachium of the inferior colliculus; AR = acoustic radiation.

To facilitate understanding of the extracted auditory tracts, we individually illustrated them in sub-figures within Fig. 4. These panels were arranged from peripheral to cortical regions in a top-to-bottom, left-to-right sequence. For consistency, the same layout applied to Figs. 5, 6, and 7, which depict the developmental trajectories of NDI, RD, and FA, respectively. Note that the CO-CN tracts were excluded from our analysis owing to significant noise in the peripheral microstructural maps, making reliable data interpretation infeasible.
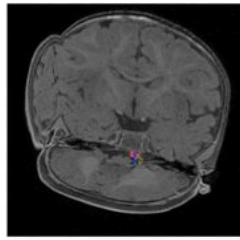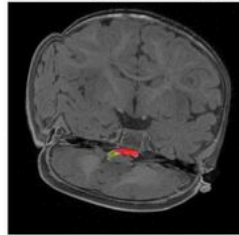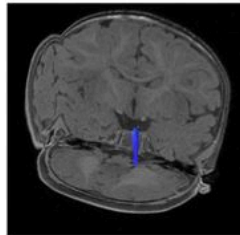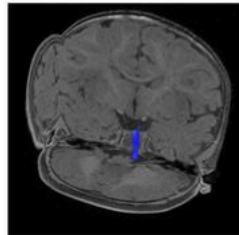
CN_L-SOC_L

CN_L-SOC_R
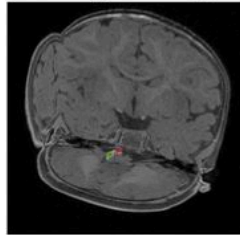
CN_R-SOC_R

CN_R-SOC_L

CN_L-IC_L

SOC_L-IC_L
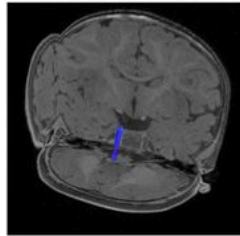
CN_R-IC_R
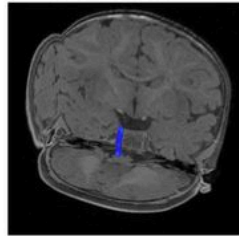
SOC_R-IC_R
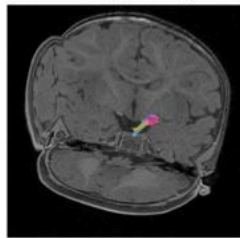
BIC_L
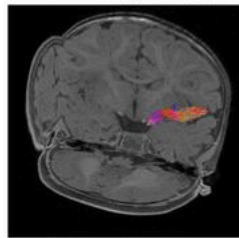
AR_L

BIC_R
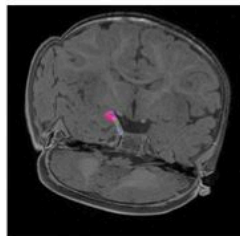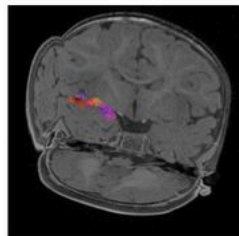
AR_R

Figure 4. Extracted auditory tracts from dMRI data of a 6-month-old infant. Detailed visualization highlights the small size and complex structure of auditory tracts within the brainstem. (Abbreviations: L=left; R=right; **CN=cochlear nucleus**; **SOC=superior olivary complex**; **IC=inferior colliculus**; **BIC=brachium of the inferior colliculus**; **AR=acoustic radiation**.)

$p = 6.9066e - 17, r^2 = 0.8211$

$\mathrm{CN_L\text{-}SOC_L}$

$p = 2.0055e - 19, r^2 = 0.9319$

$\mathrm{CN_L\text{-}SOC_R}$

$p = 3.3939e - 12, r^2 = 0.8747$

$\mathrm{CN_R\text{-}SOC_R}$

$p = 3.6559e - 24, r^2 = 0.9032$

$\mathrm{CN_R\text{-}SOC_L}$

$p = 1.6478e - 09, r^2 = 0.9013$

$\mathrm{CN_L\text{-}IC_L}$

$p = 6.9718e - 08, r^2 = 0.8110$

$\mathrm{SOC_L\text{-}IC_L}$

$p = 3.1714e - 12, r^2 = 0.7675$

$\mathrm{CN_R\text{-}IC_R}$

$p = 9.8799e - 11, r^2 = 0.8038$

$\mathrm{SOC_R\text{-}IC_R}$

$p = 2.9007e - 25, r^2 = 0.9410$

$\mathrm{BIC_L}$

$p = 3.2836e - 26, r^2 = 0.9254$

$\mathrm{AR_L}$

$p = 1.4384e - 16, r^2 = 0.9055$

$\mathrm{BIC_R}$

$p = 7.8452e - 26, r^2 = 0.8950$

$\mathrm{AR_R}$
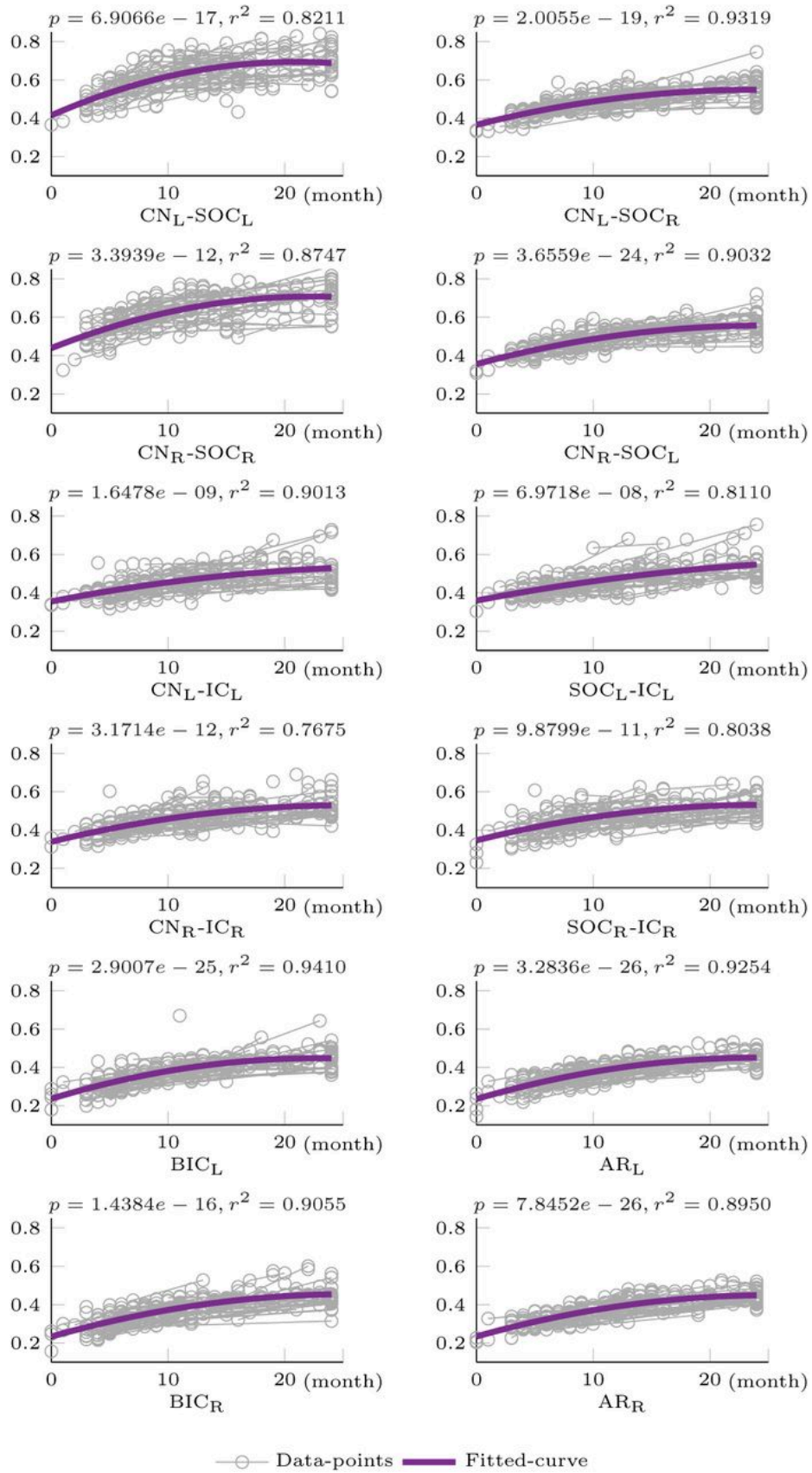
Data-points — Fitted-curve

Figure 5. Developmental trajectories of NDI with fitted curves and data points. NDI values gradually increase from birth to 24 months, exhibiting higher neurite density in brainstem regions compared to cortical regions across both hemispheres.
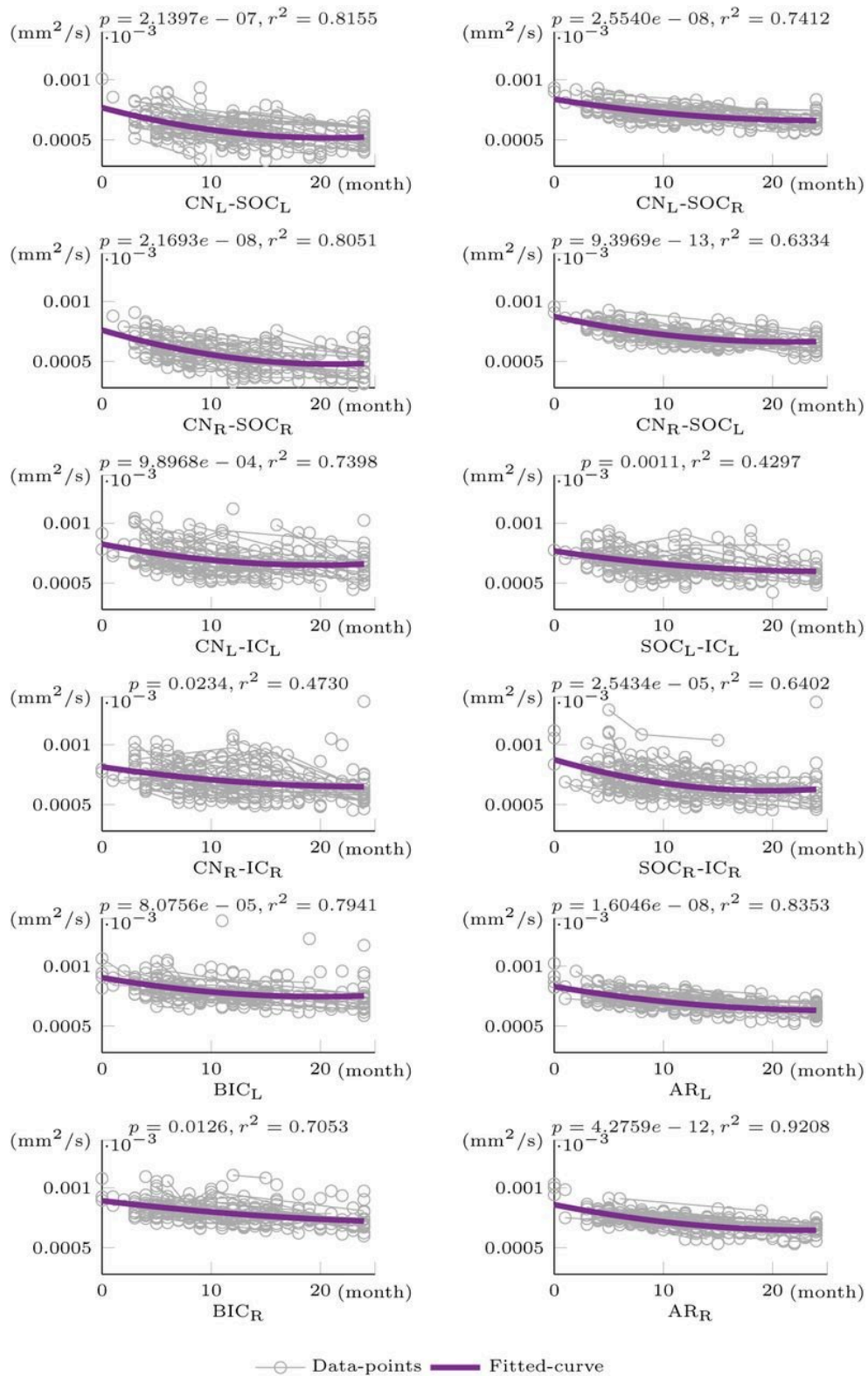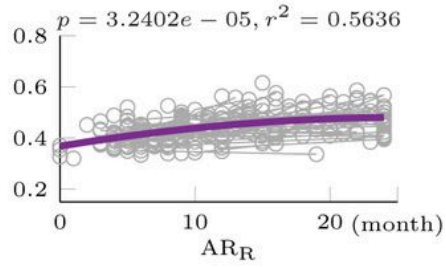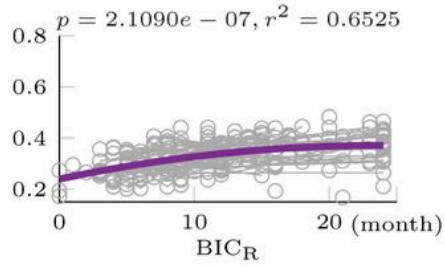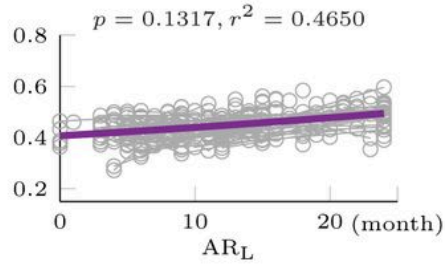
Figure 6. Developmental trajectories of RD with fitted curves and data points. RD values decrease from birth to 24 months in both hemispheres, demonstrating higher myelination near the CN and lower myelination near the PAC.

The NDI ranges from 0 to 1, with values approaching 1 indicating higher neurite density. As illustrated in Fig. 5, the fitted NDI curves for all auditory tracts display a steady increase from birth to 24 months. At birth, tracts situated in brainstem regions exhibit higher maturity levels than those in cortical regions, along the peripheral-to-cortical axis. This pattern aligns with previously proposed developmental progressions of white matter, which follow the direction of information flow[91]. Notably, the developmental trajectories reveal marked asynchrony, with tracts closer to peripheral regions maturing earlier than those nearer to PAC. This finding underscores the staggered timeline of auditory system maturation across infancy.

The inverse of RD reflects myelination status, such that lower RD values indicate better myelination. As illustrated in Fig. 6, RD trajectories gradually decrease over time, closely mirroring the patterns observed in NDI. RD, similar to NDI, shows better development in tracts closer to CN compared to those near the PAC.

The DTI model underlying RD, however, exhibits notable limitations, especially its inability to characterize crossing fibers[68][92][93][94][95]. Consequently, RD-based assessments may be less accurate than NDI (derived from the NODDI model). This limitation becomes more pronounced when using FA, which generally struggles to characterize white matter microstructure in brainstem regions rich in crossing fibers. As shown in Fig. 7, the contralateral CN-SOC exhibits marked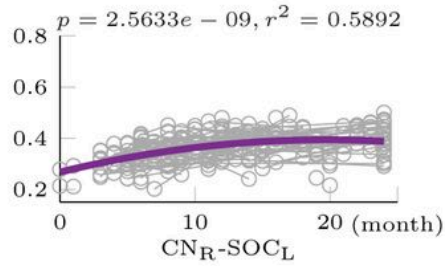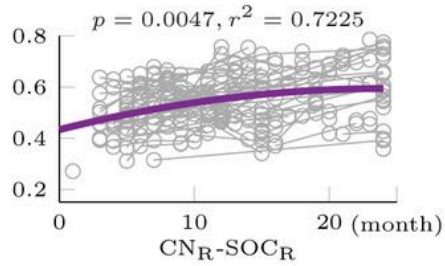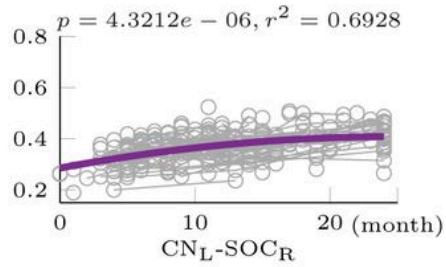ly lower FA values compared to the acoustic radiation (AR) and ipsilateral CN-SOC. These FA trajectories do not align with their NDI or RD counterparts, underscoring the challenges in using FA to represent microstructural changes in regions with complex fiber configurations. The NDI values in auditory tracts exhibited significant correlations with fine-motor skills and expressive language t-scores from the MSEL tests (see Tables 3 and 4). We used a LMM with a quadratic fit, adjusting all p-values for multiple comparisons across tracts via the Benjamini-Hochberg procedure[96].

$p = 9.1554e - 06, r^2 = 0.7165$ — $\text{CN}_\text{L}\text{-SOC}_\text{L}$

$p = 4.3212e - 06, r^2 = 0.6928$ — $\text{CN}_\text{L}\text{-SOC}_\text{R}$

$p = 0.0047, r^2 = 0.7225$ — $\text{CN}_\text{R}\text{-SOC}_\text{R}$

$p = 2.5633e - 09, r^2 = 0.5892$ — $\text{CN}_\text{R}\text{-SOC}_\text{L}$

$p = 3.1779e - 06, r^2 = 0.5825$ — $\text{CN}_\text{L}\text{-IC}_\text{L}$

$p = 7.9209e - 06, r^2 = 0.3572$ — $\text{SOC}_\text{L}\text{-IC}_\text{L}$

$p = 7.0501e - 05, r^2 = 0.4851$ — $\text{CN}_\text{R}\text{-IC}_\text{R}$

$p = 1.6005e - 10, r^2 = 0.5485$ — $\text{SOC}_\text{R}\text{-IC}_\text{R}$

$p = 1.0142e - 07, r^2 = 0.4330$ — BIC_L

$p = 0.1317, r^2 = 0.4650$ — AR_L

$p = 2.1090e - 07, r^2 = 0.6525$ — BIC_R

$p = 3.2402e - 05, r^2 = 0.5636$ — AR_R
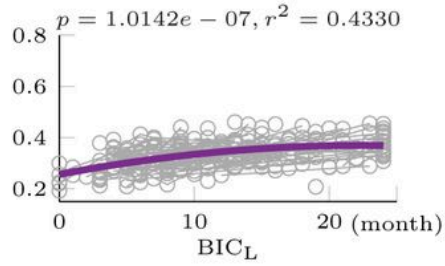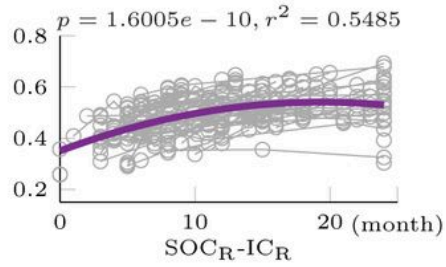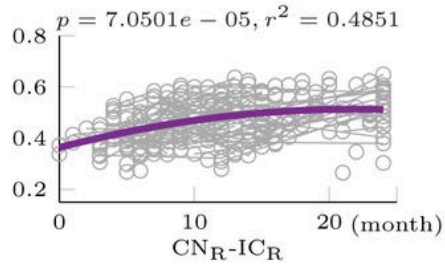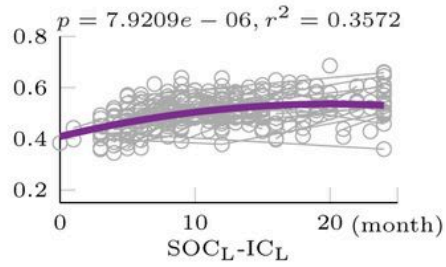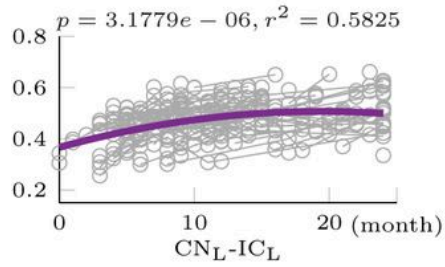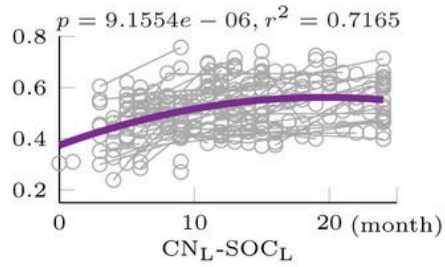
Data-points ○   Fitted-curve ——

Figure 7. Developmental trajectories of FA with fitted curves and data points. The trajectories in both hemispheres show lower FA in the contralateral CN-SOC compared to the AR and ipsilateral CN-SOC. These patterns reflect the limitations of FA in accurately characterizing white matter microstructure in regions with crossing fibers.

Fine motor t-scores	p-value	r^2
AR_L*	0.019	0.047
AR_R*	0.029	0.091
CN_R-IC_R*	0.025	0.050
CN_R-SOC_R*	0.015	0.135

Table 3. Significant correlations between auditory tract NDI values and fine-motor skills t-scores from the MSEL tests.

Expressive language t-scores	p-value	r^2
BIC_L**	0.006	0.349
BIC_R**	0.008	0.402
CN_L-IC_L*	0.013	0.333
CN_R-IC_L*	0.013	0.347

Table 4. Significant correlations between auditory tract NDI values and expressive language t-scores from the MSEL tests.

For fine-motor t-scores, statistically significant correlations ($p < 0.05$) emerged with several auditory tracts, including the bilateral AR, CN_R-IC_R, and CN_R-SOC_R. Nevertheless, these models showed relatively low r-squared scores (below 0.15), suggesting limited explanatory power. This finding implies that, while the auditory tracts do appear to support fine-motor skill development, other systems, such as motor or sensorimotor, may play a more prominent role. Further investigation is needed to clarify these relationships and underlying mechanisms.

In contrast, highly significant correlations were found between NDI values of auditory tracts and expressive language t-scores, specifically for the bilateral brachium of the inferior colliculus (BIC) ($p < 0.01$). Additionally, significant correlations were observed with the CN_L-IC_L and CN_R-IC_L tracts ($p < 0.05$), although both tracts did not

reach the same level of statistical significance as the BIC. All four tracts exhibited higher *r*-squared scores (*r*-squared> 0.3), indicating a moderate explanatory power of auditory systems for expressive language abilities.

These findings underscore the significant contribution of the auditory system to expressive language. The development of expressive language relies on the fine-motor control of speech-specific articulators, such as the tongue, lips, and vocal cords, indicating that the auditory system's influence is closely linked to these motor functions. Nevertheless, the roles of visual, motor, somatosensory, and sensorimotor systems in supporting speech production should not be overlooked, as they also play crucial roles in this complex cognitive domain. Further research is needed to elucidate the interactions and underlying mechanisms among these systems in the development of language skills.

3. Discussion

This study presents a novel toolbox for extracting auditory tracts in infants, providing a robust method to characterize white matter microstructural changes during development. By modeling the gradual and continuous maturation trajectories of these auditory tracts from birth to 24 months, we identified significant correlations between auditory tract NDI values and both *fine-motor skills* and *expressive language t*-scores from the MSEL tests. Notably, these findings offer valuable insights into the intertwined development of sensory and motor systems underlying speech acquisition, particularly in the context of perceptual reorganization, and highlight the importance of investigating how early white matter maturation may contribute to emerging speech abilities.

3.1. A robust framework for auditory tract extraction

Research on infant neuroimaging has long faced challenges in data acquisition, processing, and analysis[69][97]. Despite continuous advancements in data collection and the development of numerous processing and analysis tools[68][79][80][98][99][100][101][102][103][104][105][106], extracting auditory tracts in infants remains particularly difficult. In previous studies, such extraction often required specimen scanning or ultra-high-field scanners[74][75][76], and was limited to only a few of the 14 auditory tracts.

To address these limitations, we introduced *NeoAudi Tract* (NAT), a framework specifically developed to extract the full set of auditory tracts, spanning peripheral, subcortical, and cortical regions, from 3T HARDI data. NAT was designed to accommodate significant variability in infant MRI data, with a core emphasis on maximizing registration robustness. The key contributions of the NAT framework, which enable robust auditory tract extraction, include: (1) An auditory tract atlas constructed from the Human Connectome Project (HCP) dataset[107], offering high-quality anatomical references; (2) The use of high-spatial- and high-temporal-resolution UNC 4D infant templates[103], to preliminarily normalize brain orientation and field of view (FOV); and (3) The integration of tissue and brainstem segmentation maps, which provide additional anatomical constraints to accurately align cortical and brainstem regions in separate registration branches. Because prior processing steps often retain neck structures in

the FOV[99], a two-branch registration framework is essential for handling the resulting variability in neck size, ensuring accurate alignment.

Collectively, these design elements enable NAT to achieve accurate alignment of both cortical and brainstem nuclei across different developmental periods, thereby facilitating the extraction of the full set of auditory tracts. Using these extracted tracts, we observed a progressive increase in tract size and streamline density, reflecting a gradual and continuous developmental course from birth to 24 months. This observation is further supported by the modeled developmental trajectories, which provide quantitative evidence of ongoing white matter maturation throughout early infancy.

The NDI, RD, and FA trajectories for each tract exhibit steady increases or decreases over the 24-month period. Noticeably, tracts closer to peripheral regions exhibit higher maturity compared to those near the PAC, as indicated by the NDI and RD trajectories. However, FA values reveal pronounced differences in maturity levels between peripheral and cortical tracts. This discrepancy likely arises from the limitations of the DTI model in representing crossing fibers[68][92][93][94][95], especially within the brainstem regions where fiber crossing is more prevalent. These findings underscore the importance of using high-quality imaging data, such as HARDI, and advanced diffusion models like NODDI. By offering more reliable microstructural information, these techniques can more accurately characterize the underlying neural substrate changes, thereby refining our understanding of early neurodevelopment.

Despite its overall success, NAT has certain limitations, as reflected in an average DICE score of approximately 0.8 for nuclei alignment. In particular, the low signal-to-noise ratio (SNR) in peripheral regions, coupled with the structural complexity of the brainstem, poses challenges for precisely extracting small tracts such as the cochlear nerve and CN–SOC pathways. Future improvements in dMRI acquisition, including higher spatial and angular resolution, as well as advancements in extraction methods, will be critical to overcoming these difficulties. Additionally, constructing age-specific auditory tract atlases would further enhance extraction accuracy and reliability by better accounting for developmental variations across infancy.

3.2. A potential role of the auditory system in speech production

The auditory system supports the perception of acoustic stimuli by converting speech vibrations into electrical signals and enabling subsequent analyses of spectral, intensity, temporal, and spatial features[82][108]. However, speech inherently involves both acoustic and articulatory dimensions[109][110], with activity coordination in sensory and motor systems[65]. Recent research has therefore examined not only how the auditory or motor system independently influences speech perception[22][32], but also how the sensorimotor system integrates these processes[20][45]. Investigators emphasize that both sensory and motor experiences are essential for effective learning[53][54][55].

This raises a critical question: How do the auditory and motor systems develop in tandem to support speech acquisition, especially in the context of perceptual reorganization? While this question is fundamental to

understanding the developmental relationship between sensory and motor systems for functional integration, it remains unresolved.

Current exploration of this topic still faces challenges in characterizing those tiny and complex nuclei structures in peripheral and brainstem regions[68]. To investigate the role of the auditory system in speech acquisition, we developed NAT and examined correlations between auditory tract maturation and four domains of the MSEL: visual reception, fine-motor skills, receptive language, and expressive language. Among these domains, the NDI values of auditory tracts showed statistically significant correlations with t-scores in fine-motor skills and expressive language, suggesting a link between auditory processing and speech production. Our findings, along with those highlighting the influence of the motor system on speech perception[20][45], raise the possibility that the development of speech perception and production is intertwined, pointing to further research into the integrated development of sensory and motor systems.

Despite the repeatedly reported link between speech perception and production in infants[18][35][42][44], *auditory–motor associations may not emerge innately*[48]. Instead, recent research suggests that postnatal sensorimotor experiences facilitate the establishment of these associations[111][112], forming a basis for imitation[50][52][113]. However, the origin of imitation remains a topic of heated debates[114][115][116][117][118][119][120][121][122][123][124][125][126][127].

Once these sensory–motor associations are formed, sensory input can simultaneously activate motor regions[128][129], potentially driving plastic changes in both auditory and motor networks underlying speech acquisition[57]. During the refinement of neural connectivity, the auditory and motor systems gradually become more attuned, contributing to the sharpening of infants' sensitivity to their native language. One more specific hypothesis is that the auditory system may influence perceptual reorganization via mediation by the motor system. However, further investigation is needed to clarify the precise mechanisms underlying how auditory and motor system development interact to support early speech activities.

Among these auditory tracts, we found no significant correlation with receptive language t-scores from the MSEL tests. One possible explanation may lie in the emphasis on semantic comprehension in the test items, which are more likely to engage ventral language pathways that map sound to meaning[61][110][130]. Consequently, these semantic skills could be less dependent on the specific auditory tracts examined in our study.

In light of this, future research would expand NAT's focus beyond the auditory system to include additional systems, such as sensorimotor, visual, and motor tracts[131][132], to gain a more comprehensive understanding of how interconnected neural networks support speech acquisition and cognitive development during early infancy. Such an integrative approach may reveal how ventral and dorsal language pathways, along with additional sensory and motor pathways, collectively shape both receptive and expressive language outcomes.

4. Concluding remarks

We propose a novel toolbox, *NeoAudi Tract* (NAT), for extracting auditory tracts in infants. By charting their maturation trajectories, we identified statistically significant correlations between the NDI values of these tracts and *t*-scores for *fine-motor skills* and *expressive language* from the MSEL tests, thereby supporting the linked development of speech perception and production. We hypothesize that speech perception and production are mutually dependent processes, driven by the intertwined maturation of sensory and motor systems.

Beyond advancing our understanding of typical auditory tract maturation, NAT also holds promise for investigating developmental deviations in hearing-impaired infants. Studies have demonstrated that early auditory implants can significantly improve speech performance and language-learning outcomes[133][134][135][136], although the optimal timing and implantation strategy remain to be fully established. By uncovering both typical and atypical maturation trajectories in hearing-impaired and congenitally deaf infants[137][138][139], NAT can provide critical insights to inform clinical decision-making and predict postoperative outcomes.

In line with the paradigm shift from studying isolated brain regions to examining interconnected networks[58][61], cognitive functions are increasingly regarded as emergent properties of brain-wide interactions[58][59][140]. This perspective underscores the need to investigate how specific neural systems, such as the auditory and motor systems, develop and interact to support behavioral outcomes[132]. Our results indicate that the maturation of auditory tracts is closely associated with speech production within the context of motor system development, providing valuable insights into the plastic changes in white matter that integrate functionally segregated regions and underpin cognitive behaviors. Furthermore, this work highlights the potential of task-free, longitudinally applicable dMRI data from a 3T scanner — capable of simultaneously characterizing multiple systems — to advance our understanding of speech acquisition mechanisms. Looking ahead, future investigation will benefit from interdisciplinary collaboration across fields such as linguistics, neuroscience, psychology, neuroimaging, medicine, and computer science[2]. Such efforts will ultimately deepen our knowledge of how neural substrates develop to subserve early language and cognitive development.

5. Method

To reliably extract auditory tracts from infant dMRI data, we first constructed a high-quality atlas of auditory tracts using HCP adult data[107], then employed our proposed toolbox for processing infant sMRI and dMRI data[99], and finally designed a minimal processing pipeline to ensure accurate registration when aligning adult templates with infant data. The following sections will introduce the main framework of NAT (Section 4.1), the procedures for constructing the adult auditory tract atlas (Section 4.2), and the minimal processing steps for infant sMRI (Section 4.3) and dMRI data (Section 4.4).

5.1. NAT framework

As illustrated in Fig. 8, NAT comprises two main components: (1) *atlas preparation* and (2) *tract extraction*. NAT is specifically designed to improve registration accuracy, ensuring reliable alignment between infant data and adult templates. By simply replacing the atlas and segmented ROI masks, NAT can be easily adapted to extract any tract in subjects at any age period, offering a flexible solution for a broad range of developmental neuroimaging studies.
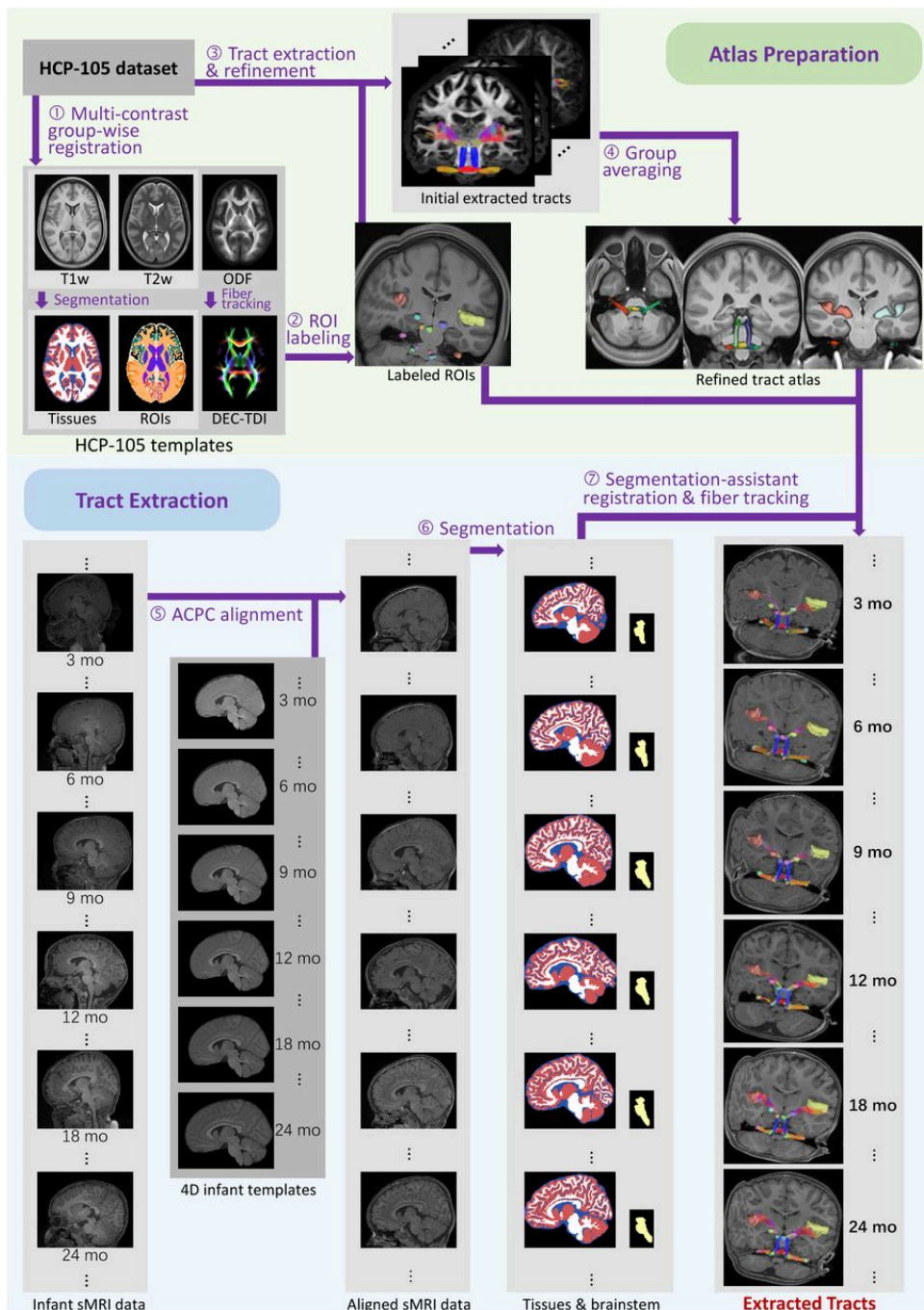
Figure 8. Overview of the NAT framework, which comprises two main components: (1) *atlas preparation* and (2) *tract extraction*. (1) Atlas preparation involves creating a high-resolution atlas of auditory tracts, including key nuclei such as the cochlea (CO), cochlear nucleus (CN), superior olivary complex (SOC), inferior colliculus (IC), medial geniculate body (MGB), and primary auditory cortex (PAC; Heschl's gyrus), as well as tract masks. (2) Tract extraction utilizes precise segmentation of infant brain tissues and ROIs to support the registration framework, enabling accurate delineation of tract anatomy.

In the first part, *atlas preparation*, we employed a high-quality MRI dataset from HCP[107], which enabled us to delineate the minute nuclei in auditory pathways. Below, we detail four core procedures: **(1.1)** We first constructed group-wise, multi-modality MRI templates from 105 subjects[141]. **(1.2)** Using complementary information revealed in these multi-modality MRI templates, one experienced neuroradiologist (15 years of experience) labeled the initial and terminal regions of the auditory tracts. Another neuroradiologist (29 years of experience) then reviewed these labels to ensure accuracy. **(1.3)** The labeled ROIs in the template space were aligned to each subject's space to facilitate the extraction of auditory tracts. **(1.4)** The extracted tracts in each subject space were subsequently aligned back to the template space and group-averaged, resulting in an initial tract atlas. We used this initial tract atlas to refine the tract extraction in Step (1.3), and the newly extracted tracts were employed to update the tract atlas in Step (1.4). These two steps were repeated iteratively, thereby refining the tract atlas with each iteration.

In the second part of NAT, *tract extraction*, we performed three core procedures:

(2.1) We first aligned the infant sMRI data with the UNC 4D infant templates for anterior commissure and posterior commissure (ACPC) alignment[103], which facilitates subsequent steps, including tissue segmentation and registration. **(2.2)** We then segmented infant tissues and ROI maps, which were incorporated into the registration to improve robustness. **(2.3)** Finally, we combined anatomical information from both the aligned atlas and segmentation maps to ensure the reliability of the extracted auditory tracts.

5.2. Atlas preparation and refinement

Given that auditory nuclei are very small and structurally complex, neuroradiologists have to locate them using high-quality T1-weighted (T1w), T2-weighted (T2w), and dMRI data to fully exploit their complementary information[68]. Therefore, we employed 105 subjects from the HCP dataset to construct multi-modality templates for labeling these nuclei efficiently[107][141]. Instead of using raw data, we employed the processed sMRI and dMRI data provided by HCP[142], which required only a few additional processing procedures as detailed below. It is worth noting that we directly employed the 0.7 mm^3 T1w and T2w data, rather than the 1.25 mm^3 data accompanying the processed dMRI data, to preserve higher spatial resolution information. We aligned the T1w and T2w data during ACPC alignment, ensuring consistent orientation across modalities.

As shown in Fig. 9, we constructed both the sMRI and dMRI (*i.e.*, fiber orientation distribution function (ODF)) templates for labeling auditory nuclei. To build T1w and T2w templates, we employed the *antsMultivariateTemplateConstruction2* script from the ANTs toolbox[143][144], which iteratively generates and optimizes candidate templates by incorporating multi-modality information[145]. Before constructing the ODF template, we modified our previously proposed dMRI processing pipeline[99] to better accommodate peripheral and brainstem regions. Specifically, we first estimated the response function for spherical deconvolution using the *dhollander* algorithm[146], then chose the *csd* approach for generating constrained spherical deconvolution ODFs[147]. To build ODF template, we employed the *population template* tool from MRTrix3[148]. In order to properly include

peripheral tracts, we dilated the brain masks before normalizing ODFs, thereby ensuring these regions were not inadvertently excluded.
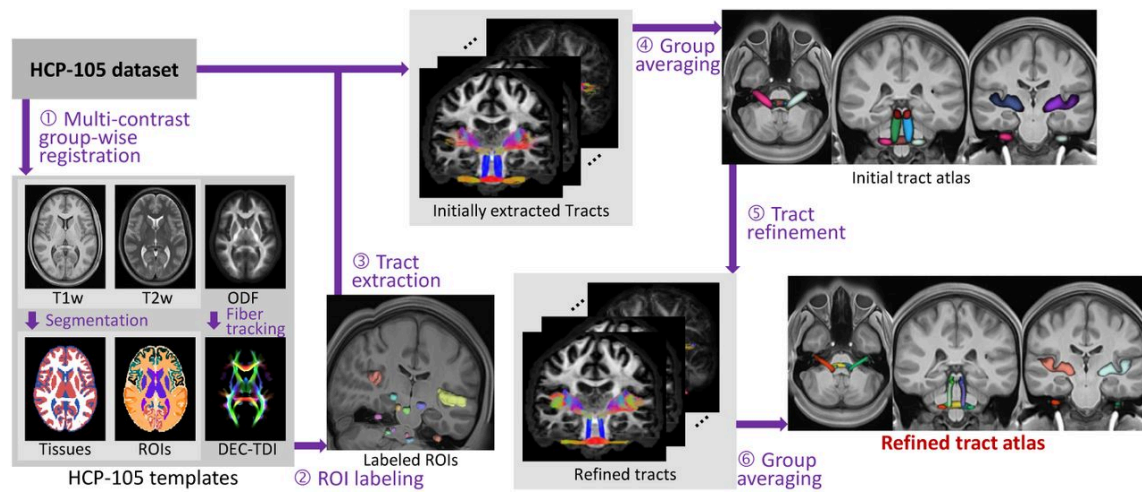

Figure 9. Preparation of high-resolution templates and auditory tract atlas for adults. Labeled ROIs in the template space were used to extract initial tracts, which were then utilized to create tract probability maps, forming a preliminary tracts atlas. This atlas was subsequently refined to enhance the precision of auditory tract extraction, resulting in a more accurate tracts atlas.

Once the T1w, T2w, and ODF templates were constructed, we aligned the T1w template to the ODF template using ANTs rigid registration[149]. We then applied deep-learning–based segmentation methods to the T1w template in order to obtain tissue maps and ROIs (including Desikan–Killiany–Tourville (DKT) regions as well as subcortical and cerebellar areas)[150][151]. Next, the T2w template, along with tissue and ROI maps, was warped to the dMRI data space using the same transformation matrix derived from the T1w-template registration. In addition, we used the ODF template to generate a directionally-encoded color track density imaging (DEC-TDI) map, following the configurations described in[68]. Finally, experienced neuroradiologists delineated the auditory nuclei by jointly examining the T1w, T2w, DEC-TDI, tissues, and DKT-ROI maps.

The labeled auditory ROIs were then warped to each subject's dMRI space, serving as the initial and terminal regions for fiber tracking. These aligned ROIs enabled the extraction of initial auditory tracts in the individual dMRI space. All extracted tracts were subsequently aligned back to the template space for group averaging, resulting in an initial tract atlas. Because the initial auditory tracts might include outlier streamlines, we further used the initial auditory tract atlas to discard streamlines lying outside the aligned atlas. These refinement procedures can be repeated iteratively; in this work, we refined the initial atlas only once, as it already demonstrated the adequate accuracy.

5.3. Minimal processing for sMRI data

During the first two postnatal years, the infant brain undergoes rapid growth in size and ongoing myelination, leading to substantial changes in gray matter (GM) and white matter (WM). Consequently, sMRI data of this period exhibit large variations in intensity distributions[106], posing significant challenges for accurate brain tissue segmentation and registration. Hence, robust sMRI data processing is crucial for leveraging the adult atlas to extract auditory tracts from infant neuroimaging data. Building on our previously proposed tools for infant neuroimaging processing[68][98][101][104], we obtained brain tissue and ROI maps from neonates up to 24-month-old infants. This minimal processing framework helps ensure reliable alignment between infant sMRI data and the adult templates, forming the foundation for subsequent auditory tract extraction.

5.3.1. sMRI data preprocessing

We performed sMRI data preprocessing using FSL[152], ANTs[153], and MRtrix3[148]. First, all sMRI data underwent N4 bias field correction to address intensity inhomogeneities[153]. We then obtained a rough brain mask by rigidly aligning each T1w data to the corresponding age-specific template[103], which allowed for a rough skull stripping and removal of facial and neck tissues. Next, the skull-stripped T1w data served as a reference for ACPC alignment, so that improving the robustness of subsequent brain tissue segmentation and non-rigid registration. Finally, for each subject, the T2w data were rigidly aligned to the T1w data using *flirt* in FSL, ensuring consistent orientation across both modalities.

Subsequently, we employed our previously proposed deep learning models to segment infant brain tissues[101][104]. These models leverage the intensity-invariant anatomical features to accommodate substantial variations in intensity distributions characteristic of the rapid development. Unlike prior studies that relied on age-specific models[154], our single-model approach enabled precise and longitudinally consistent tissue segmentation across a broad age range[104]. Both tissue and brainstem segmentation maps then served as anatomical guidance for accurately aligning infant sMRI data with adult templates, ensuring robust registration despite the considerable variations in intensity distribution.

5.3.2. Two-branch registration framework

The auditory tract extraction poses two major challenges for the alignment: (1) auditory tracts traverse peripheral, subcortical, and cortical regions, and (2) the lower portions of the brainstem exhibit large variations in the processed neuroimaging data. Consequently, it is difficult to simultaneously align both the cortical and brainstem regions of adult templates to infant sMRI data. To address this issue, we developed a two-branch registration framework that separately aligns the cortical areas and the brainstem, as illustrated in Fig. 10. This design allows for more accurate alignment of both regions despite their distinct anatomical and developmental characteristics.
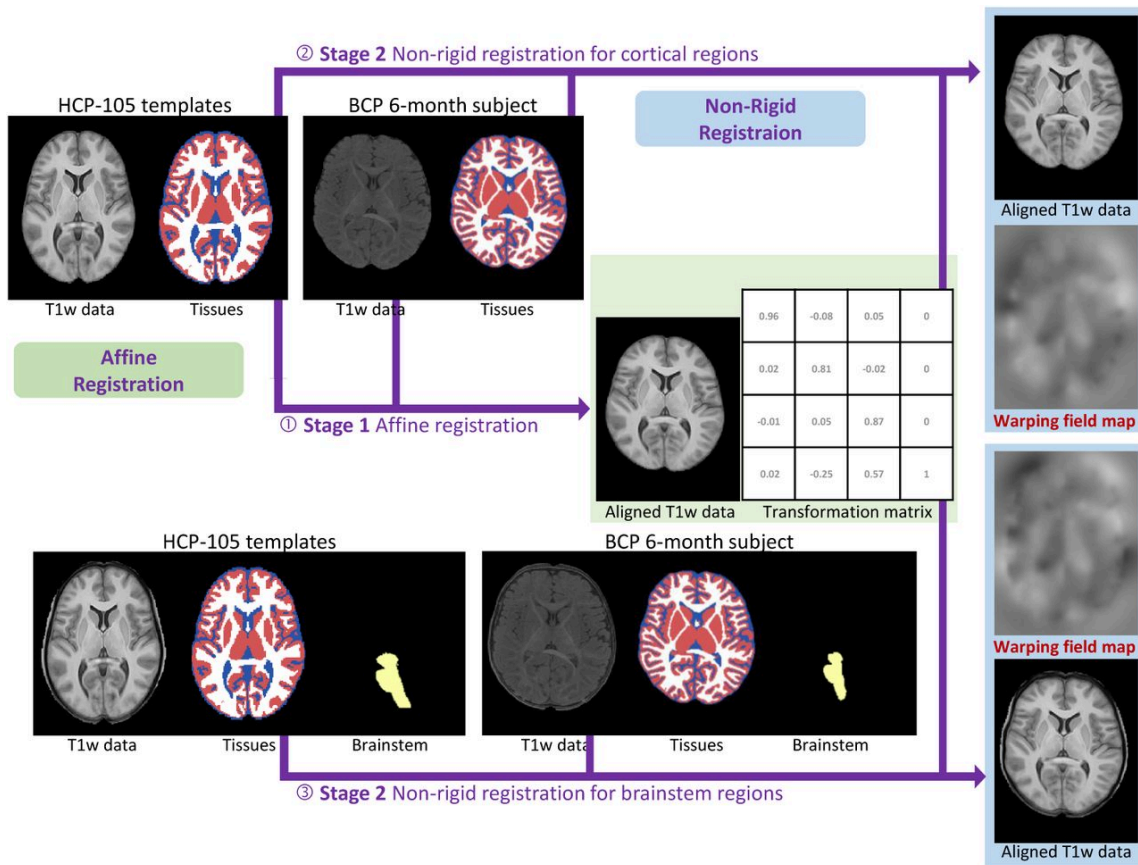
Figure 10. Two-branch registration framework for aligning adult templates with infant sMRI data. The framework utilizes both T1w and T2w data, although T2w data are not shown here for clarity. The alignment process consists of two stages: (1) Affine registration using tissue maps to adjust intensity contrasts between gray matter and white matter; (2) Dual deformable registration branches to finetune the alignment of cortical and subcortical regions separately.

Our proposed framework proceeds in two distinct stages: (1) *affine registration* and (2) *deformable registration*. *In the first stage*, there is a single branch focusing on cortical alignment. We employed skull-stripped data for affine registration of cortical regions (from adult sMRI templates to infant sMRI data), guided by the segmented tissue maps. This process yielded a transformation matrix that serves as the initial transform for the subsequent deformable registrations. *In the second stage*, two branches of deformable registration were performed to separately warp cortical and brainstem regions. For the cortical branch, tissue maps are utilized. For the brainstem branch, in addition to tissue maps, we also incorporated the brainstem map and dilated brain mask to ensure accurate normalization of the brainstem area. Finally, these two-branch warping fields effectively align both cortical and brainstem regions, laying the groundwork for reliable auditory tract extraction.

5.3.3. ROIs refinement for tracking fibers

After completing the registration steps, we obtained reference information from adult atlas. In addition to the aligned auditory ROIs and tract masks in the individual space, we also utilized tract endpoint pairs as complementary cues for refining region definitions. Specifically, we extracted the initial and terminal regions of each tract from its corresponding tract mask. The order of the initial and terminal regions was established, during the construction of the adult tract atlas, by referencing one of the 105 adult subjects using *QuickBundle*[155]. This approach helps ensure a consistent orientation of fibers (*i.e.*, initial *vs.* terminal) across subjects, thereby improving the reliability of subsequent fiber tracking and analysis.

For ROI refinement, we first combined the two endpoint regions of each tract with the corresponding auditory ROIs, then further refined them using segmentation maps, as shown in Fig. 11. This procedure aligns with the anatomically constrained tractography (ACT) framework implemented in MRTrix3[148]. Specifically, to extract auditory tracts under the ACT framework, we delineated the GM/WM interface and used it to identify intersections between this interface and the combined auditory ROIs. In line with ACT's objective, these refinement steps help ensure the fidelity of the tracked fibers.
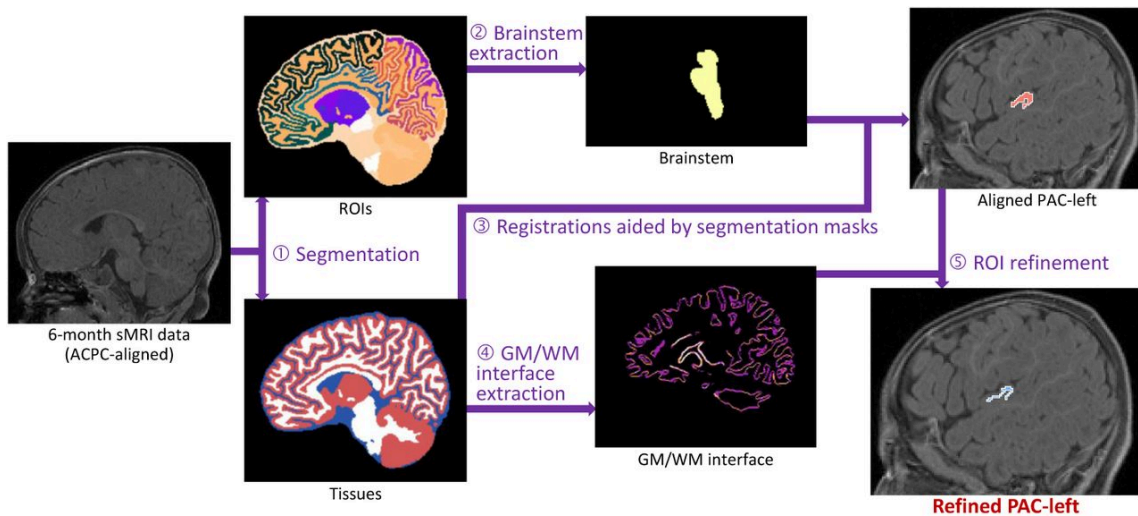

Figure 11. Deep learning based segmentation of brain tissues and DKT–based ROIs using T1w and T2w data. The segmented maps were utilized to delineate the brainstem and the interface between GM and WM. This segmentation provides consistent tissue contrast, facilitating subsequent registration processes, and allows for precise adjustment of aligned ROIs for accurate identification of auditory tracts. The refined left primary auditory cortex (PAC) demonstrates improved accuracy.

5.4. Extraction of auditory tracts

To precisely extract auditory tracts, NAT leveraged anatomical guidance from sMRI data to effectively preprocess infant dMRI data[99], thereby alleviating the spatiotemporal asynchrony of white matter development.

We employed MRtrix3, FSL, and ANTs to process the dMRI data. All data underwent bias and distortion correction[156][157][158][159], denoising[160], and co-registration[161]. Specifically, we aligned each sMRI data to the dMRI space via boundary-based registration (BBR)[162], guided by the segmented tissue maps. Subsequently, we applied rotation and correction of the B-matrix to ensure accurate streamline tracking[163]. Notably, this differs from the previous pipeline[99] in how the response function and ODF are generated (see Section 4.2 for details), catering to peripheral and brainstem regions. Rather than using a dilated brain mask, we adopted the regular brain mask to normalize the obtained ODF across GM, WM, and cerebrospinal fluid (CSF)[164], thus capturing appropriate tissue information without introducing spurious peripheral influences.

With the normalized ODF, we next utilized the aligned ROIs in the dMRI space to create three types of masks: inclusion, seed, and exclusion. The auditory tracts were then extracted individually using the *iFOD2* algorithm[165]. Specifically, we employed the combined ROIs as inclusion masks, and defined seeds only at regions intersecting the GM/WM interface to ensure biologically plausible in generating streamlines. Meanwhile, we dilated the aligned tract masks and inverted them to derive exclusion masks, thereby filtering out outlier streamlines.

Moreover, we implemented a data quality control (QC) procedure at each step to ensure the reliability of the analyses[166]. Specifically, during QC, each data sample was labeled as *pass*, *questionable*, or *fail*. We excluded *fail* data from subsequent analyses, while both *pass* and *questionable* data were retained.

The QC criteria encompassed three major aspects: (1) acquisition issues (*e.g.*, early stopping, excessive motion, blurring, and signal loss), (2) processing issues (*e.g.*, severe intensity artifacts, distortion-correction failures, misalignment, and tract extraction failures), and (3) tract attributes that were not longitudinally consistent in longitudinal charting. Data labeled *pass* showed no apparent artifacts, good alignment, and consistency across time points, whereas *questionable* datasets exhibited moderate issues in one or more of these areas. Together, *pass* and *questionable* data constituted only 42.89 % of the total dataset.

These configurations ensure that fiber tracking remains confined within valid anatomical boundaries, thereby enhancing the accuracy and consistency of the extracted tracts and ultimately ensuring the reliability of the analysis.

Statements and Declarations

This manuscript is an extended version of the abstract presented at the 2024 *International Society for Magnetic Resonance in Medicine (ISMRM) Annual Meeting*. The abstract was part of the ISMRM 2024 *Power Pitch Program* (#0240). For more details, refer to the following links:

- NAT — ISMRM Abstract Archive Link
- Infant multi-modality MRI data processing — ISMRM Abstract Archive Link
- YouTube Presentation Video

Author Contributions

F.L. and Y.W. designed the research, wrote the codes, and drafted the manuscript. F.L., J.G., and J.L. collected data, designed processing tools, and processed the data. F.L. and X.C. provided statistical analysis and interpretation of the data. Y.W., Z.W., and H.W. made contributions in the areas of anatomical delineation and data analysis. H.Z., J.F., and D.S. coordinated and supervised the whole work. All authors were involved in critical revisions of the manuscript, and have read and approved the final version.

Conflicts of Interest

The authors declare no competing financial and non-financial interests.

References

1. ^Kuhl PK. "Early language acquisition: Cracking the speech code". Nature Reviews Neuroscience. 5: 831–843 (2004).

2. a, b Kuhl PK, Gleitman L. "Opportunities and challenges for language learning and education. final workshop report". National Science Foundation, Washington, DC (2007).

3. ^Meltzoff AN, Kuhl PK, Movellan J, Sejnowski TJ. "Foundations for a new science of learning". Science. 325: 284–288 (2009).

4. ^Kuhl P, Rivera-Gaxiola M. "Neural substrates of language acquisition". Annual Review Neuroscience. 31: 511–534 (2008).

5. ^Gervain J, Mehler J. "Speech perception and language acquisition in the first year of life". Annual Review of Psychology. 61: 191–218 (2010).

6. a, b Zatorre RJ, Fields RD, Johansen-Berg H. "Plasticity in gray and white: Neuroimaging changes in brain structure during learning". Nature Neuroscience. 15: 528–536 (2012).

7. ^Kuhl PK, Damasio A. in Language 5 edn, (eds Kandel ER et al.) Principles of Neural Science 1353–1372 (McGraw Hill, New York, 2012).

8. ^Werker JF, Hensch TK. "Critical periods in speech perception: New directions". Annual Review of Psychology. 66: 173–196 (2015).

9. ^Reh RK, Hensch TK, Werker JF. "Distributional learning of speech sound categories is gated by sensitive periods". Cogn ition. 213: 104653 (2021).

10. ^Werker JF. "Phonetic perceptual reorganization across the first year of life: Looking back". Infant Behavior and Develo pment. 75: 101935 (2024).

11. ^Fedorenko E, Ivanova AA, Regev TI. "The language network as a natural kind within the broader landscape of the hu man brain". Nature Reviews Neuroscience. 1–24 (2024).

12. ^Rescorla L. "Age 17 language and reading outcomes in late-talking toddlers: Support for a dimensional perspective on language delay". Journal of Speech, Language, and Hearing Research (2009).

13. ^Kuhl PK. "Brain mechanisms in early language acquisition". Neuron. 67: 713–727 (2010).

14. ^Newman R, Ratner NB, Jusczyk AM, Jusczyk PW, Dow KA. "Infants' early ability to segment the conversational speech signal predicts later language development: A retrospective analysis". Developmental Psychology. 42: 643 (2006).

15. ^Purpura DJ, Reid EE. "Mathematics and language: Individual and group differences in mathematical language skills i n young children". Early Childhood Research Quarterly. 36: 259–268 (2016).

16. ^Marchman VA, Fernald A. "Speed of word recognition and vocabulary knowledge in infancy predict cognitive and lan guage outcomes in later childhood". Developmental Science. 11: F9–F16 (2008).

17. ^Kuhl PK, Meltzoff AN. "The bimodal perception of speech in infancy". Science. 218: 1138–1141 (1982).

18. a, b, c, dPulvermüller F, et al. "Motor cortex maps articulatory features of speech sounds". Proceedings of the National A cademy of Sciences. 103: 7865–7870 (2006).

19. a, bde Klerk CC, Johnson MH, Heyes CM, Southgate V. "Baby steps: Investigating the development of perceptual–motor couplings in infancy". Developmental Science. 18: 270–280 (2015).

20. a, b, cChoi D, Kandhadai P, Danielson DK, Bruderer AG, Werker JF. "Does early motor development contribute to speech perception?". The Behavioral and Brain Sciences. 40: e388 (2017).

21. ^Lotto AJ, Holt LL. in Chapter 16 - Speech perception: The view from the auditory system (eds Hickok G, Small SL) Neur obiology of Language 185–194 (Elsevier, 2016).

22. a, bHamilton LS, Oganian Y, Hall J, Chang EF. "Parallel and distributed encoding of speech across human auditory corte x". Cell. 184: 4626–4639 (2021).

23. ^Ghosh SS, Tourville JA, Guenther FH. "A neuroimaging study of premotor lateralization and cerebellar involvement in the production of phonemes and syllables". Journal of Speech, Language, and Hearing Research. 51: 1183–1202 (2008).

24. ^Khanna AR, et al. "Single-neuronal elements of speech production in humans". Nature. 626: 603–610 (2024).

25. ^Mitsuya T, Munhall KG. "The influence of bistable auditory feedback on speech motor control". Experimental Brain Re search. 237: 3155–3163 (2019).

26. ^Parrell B, Houde J. "Modeling the role of sensory feedback in speech motor control and learning". Journal of Speech, L anguage, and Hearing Research. 62: 2963–2985 (2019).

27. ^Guenther FH, Hickok G. "Role of the auditory system in speech production". Handbook of Clinical Neurology. 129: 161– 175 (2015).

28. ^*Silva AB, Littlejohn KT, Liu JR, Moses DA, Chang EF. "The speech neuroprosthesis". Nature Reviews Neuroscience. 1–2 0 (2024).*

29. ^*Liberman AM, Mattingly IG. "The motor theory of speech perception revised". Cognition. 21: 1–36 (1985).*

30. ^*Gallese V, Gernsbacher MA, Heyes C, Hickok G, Iacoboni M. "Mirror neuron forum". Perspectives on Psychological Scie nce. 6: 369–407 (2011).*

31. ^*Smalle EH, Rogers J, Möttönen R. "Dissociating contributions of the motor cortex to speech perception and response bi as by using transcranial magnetic stimulation". Cerebral Cortex. 25: 3690–3698 (2015).*

32. a, b*Nuttall HE, Kennedy-Higgins D, Devlin JT, Adank P. "Modulation of intra-and inter-hemispheric connectivity betw een primary and premotor cortex during speech perception". Brain and Language. 187: 74–82 (2018).*

33. ^*Assaneo MF, et al. "Spontaneous synchronization to speech reveals neural mechanisms facilitating language learnin g". Nature Neuroscience. 22: 627–632 (2019).*

34. ^*Kuhl PK. "Birds and babies: Ontogeny of vocal learning". Proceedings of the National Academy of Sciences. 121: e2405 626121 (2024).*

35. a, b*Pulvermüller F, Fadiga L. "Active perception: Sensorimotor circuits as a cortical basis for language". Nature Reviews Neuroscience. 11: 351–360 (2010).*

36. ^*Wu ZM, Chen ML, Wu XH, Li L. "Interaction between auditory and motor systems in speech perception". Neuroscience Bulletin. 30: 490–496 (2014).*

37. ^*D'Ausilio A, et al. "Listening to speech recruits specific tongue motor synergies as revealed by transcranial magnetic st imulation and tissue-Doppler ultrasound imaging". Philosophical Transactions of the Royal Society B: Biological Scien ces. 369: 20130418 (2014).*

38. ^*Nuttall HE, Kennedy-Higgins D, Devlin JT, Adank P. "The role of hearing ability and speech distortion in the facilitatio n of articulatory motor cortex". Neuropsychologia. 94: 13–22 (2017).*

39. ^*D'Ausilio A, et al. "The motor somatotopy of speech perception". Current Biology. 19: 381–385 (2009).*

40. ^*Rogers JC, Möttönen R, Boyles R, Watkins KE. "Discrimination of speech and non-speech sounds following theta-burs t stimulation of the motor cortex". Frontiers in Psychology. 5: 754 (2014).*

41. ^*Yeung HH, Werker JF. "Lip movements affect infants' audiovisual speech perception". Psychological Science. 24: 603– 612 (2013).*

42. a, b*Bruderer AG, Danielson DK, Kandhadai P, Werker JF. "Sensorimotor influences on speech perception in infancy". Pro ceedings of the National Academy of Sciences. 112: 13531–13536 (2015).*

43. ^*Choi D, Bruderer AG, Werker JF. "Sensorimotor influences on speech perception in pre-babbling infants: Replication a nd extension of Bruderer et al. (2015)". Psychonomic Bulletin & Review. 26: 1388–1399 (2019).*

44. a, b*Choi D, Dehaene-Lambertz G, Peña M, Werker JF. "Neural indicators of articulator-specific sensorimotor influences on infant speech perception". Proceedings of the National Academy of Sciences. 118: e2025043118 (2021).*

45. a, b, c*Choi D, Yeung HH, Werker JF. "Sensorimotor foundations of speech perception in infancy". Trends in Cognitive Sci ences. 27: 773–784 (2023).*

46. ∧*Kuhl PK, Ramírez RR, Bosseler A, Lin JFL, Imada T. "Infants' brain responses to speech suggest analysis by synthesis". Proceedings of the National Academy of Sciences. 111: 11238–11245 (2014).*

47. ∧*Dehaene-Lambertz G, et al. "Functional organization of perisylvian activation during presentation of sentences in pre verbal infants". Proceedings of the National Academy of Sciences. 103: 14240–14245 (2006).*

48. a, b*Imada T, et al. "Infant speech perception activates Broca's area: A developmental magnetoencephalography study". Neuroreport. 17: 957–962 (2006).*

49. ∧*Catmur C, Walsh V, Heyes C. "Associative sequence learning: The role of experience in the development of imitation an d the mirror system". Philosophical Transactions of the Royal Society B: Biological Sciences. 364: 2369–2380 (2009).*

50. a, b*Heyes C. "Imitation: Not in our genes". Current Biology. 26: R412–R414 (2016).*

51. ∧*Keven N, Akins KA. "Neonatal imitation in context: Sensorimotor development in the perinatal period". Behavioral an d Brain Sciences. 40: e381 (2017).*

52. a, b*Catmur C, Heyes C. "Mirroring 'meaningful' actions: Sensorimotor learning modulates imitation of goal-directed ac tions". Quarterly Journal of Experimental Psychology. 72: 322–334 (2019).*

53. a, b*Stoel-Gammon C. "Prelinguistic vocalizations of hearing-impaired and normally hearing subjects: A comparison of consonantal inventories". Journal of Speech and Hearing Disorders. 53: 302–315 (1988).*

54. a, b*McKyton A, Ben-Zion I, Zohary E. "Lack of automatic imitation in newly sighted individuals". Psychological Scienc e. 29: 304–310 (2018).*

55. a, b*Brunsdon VE, Bradford EE, Smith L, Ferguson HJ. "Short-term physical training enhances mirror system activation t o action observation". Social Neuroscience. 15: 98–107 (2020).*

56. ∧*Friston K. "Learning and inference in the brain". Neural Networks. 16: 1325–1352 (2003).*

57. a, b*Fields RD. "White matter in learning, cognition and psychiatric disorders". Trends in Neurosciences. 31: 361–370 (20 08).*

58. a, b, c*Park HJ, Friston K. "Structural and functional brain networks: From connections to cognition". Science. 342: 12384 11 (2013).*

59. a, b*Thiebaut de Schotten M, Forkel SJ. "The emergent properties of the connected brain". Science. 378: 505–510 (2022).*

60. ∧*Perani D, et al. "Neural language networks at birth". Proceedings of the National Academy of Sciences. 108: 16056–16 061 (2011).*

61. a, b, c*Dick AS, Bernal B, Tremblay P. The language connectome: New pathways, new concepts. The Neuroscientist. 20, 4 53–467 (2014).*

62. ∧*Huang H, Vasung L. Gaining insight of fetal brain development with diffusion MRI and histology. International Journa l of Developmental Neuroscience. 32, 11–22 (2014).*

63. ∧*Friederici AD. White-matter pathways for speech and language processing. Handbook of Clinical Neurology. 129, 177– 186 (2015).*

64. ∧*Maffei C, Soria G, Prats-Galino A, Catani M. Imaging white-matter pathways of the auditory system with diffusion im aging tractography. Handbook of Clinical Neurology. 129, 277–288 (2015).*

65. <u>a</u>, <u>b</u>*Friederici AD, Chomsky N, Berwick RC, Moro A, Bolhuis JJ. Language, mind and brain. Nature Human Behaviour. 1, 713–722 (2017).*

66. <u>^</u>*Ouyang M, Dubois J, Yu Q, Mukherjee P, Huang H. Delineation of early brain development from fetuses to infants with diffusion MRI and beyond. NeuroImage. 185, 836–850 (2019).*

67. <u>^</u>*Silver E, et al. A systematic review of MRI studies of language development from birth to 2 years of age. Developmental Neurobiology. 81, 63–75 (2021).*

68. <u>a</u>, <u>b</u>, <u>c</u>, <u>d</u>, <u>e</u>, <u>f</u>, g, <u>h</u>, <u>i</u>, j*Wang Y, et al. Impact of inner ear malformation and cochlear nerve deficiency on the development of auditory-language network in children with profound sensorineural hearing loss. eLife. 12, e85983 (2023).*

69. <u>a</u>, <u>b</u>, <u>c</u>, <u>d</u>*Qiu A, Mori S, Miller MI. Diffusion tensor imaging for understanding brain development in early life. Annual Review of Psychology. 66, 853–876 (2015).*

70. <u>^</u>*Moore JK, Perazzo LM, Braun A. Time course of axonal myelination in the human brainstem auditory pathway. Hearing Research. 87, 21–31 (1995).*

71. <u>^</u>*Moore J, Guan Y, Shi S. Axogenesis in the human fetal auditory system, demonstrated by neurofilament immunohistochemistry. Anatomy and embryology. 195, 15–30 (1996).*

72. <u>^</u>*Litovsky R. Development of the auditory system. Handbook of Clinical Neurology. 129, 55–72 (2015).*

73. <u>^</u>*Moore R, et al. Antenatal determination of fetal brain activity in response to an acoustic stimulus using functional magnetic resonance imaging. Human Brain Mapping. 12, 94–99 (2001).*

74. <u>a</u>, <u>b</u>, <u>c</u>*Sitek KR, et al. Mapping the human subcortical auditory system using histology, postmortem MRI and in vivo MRI at 7T. eLife. 8, e48932 (2019).*

75. <u>a</u>, <u>b</u>*Zanin J, et al. Using diffusion-weighted magnetic resonance imaging techniques to explore the microstructure and connectivity of subcortical white matter tracts in the human auditory system. Hearing Research. 377, 1–11 (2019).*

76. <u>a</u>, <u>b</u>*Epprecht L, et al. Human cochlear nucleus on 7 tesla diffusion tensor imaging: Insights into micro-anatomy and function for auditory brainstem implant surgery. Otology & Neurotology. 41, e484–e493 (2020).*

77. <u>^</u>*Huang Z, et al. Not, P. (ed.) Accelerating dwi data acquisition: Reconstruction using graph-driven denoising diffusion probabilistic model. (ed.Not, P.) 2024 IEEE International Symposium on Biomedical Imaging (ISBI), 1–5 (IEEE, 2024).*

78. <u>a</u>, <u>b</u>, <u>c</u>*Grotheer M, et al. White matter myelination during early infancy is linked to spatial gradients and myelin content at birth. Nature Communications. 13, 997 (2022).*

79. <u>a</u>, <u>b</u>*Shi F, et al. Infant brain atlases from neonates to 1-and 2-year-olds. PloS One. 6, e18746 (2011).*

80. <u>a</u>, <u>b</u>, <u>c</u>*Howell BR, et al. The UNC/UMN baby connectome project (BCP): An overview of the study design and protocol development. NeuroImage. 185, 891–905 (2019).*

81. <u>^</u>*Mullen E. Mullen scales of early learning. American Guidance Service (1995).*

82. <u>a</u>, <u>b</u>, <u>c</u>*Pickles JO. Auditory pathways: Anatomy and physiology. Handbook of Clinical Neurology. 129, 3–25 (2015).*

83. <u>^</u>*Malmierca MS, Hackett TA. in 9 structural organization of the ascending auditory pathway (eds Palmer AR, Rees A) The Oxford Handbook of Auditory Science: The Auditory Brain (Oxford University Press, 2010).*

84. ^Maffei C, Sarubbo S, Jovich J. Diffusion-based tractography atlas of the human acoustic radiation. Scientific Reports. 9, 4046 (2019).

85. ^Moore JK. Maturation of human auditory cortex: Implications for speech perception. Annals of Otology, Rhinology & Laryngology. 111, 7–10 (2002).

86. ^Bethlehem RA, et al. Brain charts for the human lifespan. Nature. 604, 525–533 (2022).

87. ^Zhang H, Schneider T, Wheeler-Kingshott CA, Alexander DC. NODDI: Practical in vivo neurite orientation dispersion and density imaging of the human brain. NeuroImage. 61, 1000–1016 (2012).

88. ^Le Bihan D, et al. Diffusion tensor imaging: Concepts and applications. Journal of Magnetic Resonance Imaging. 13, 534–546 (2001).

89. ^Kuznetsova A, Brockhoff PB, Christensen RH. lmerTest package: Tests in linear mixed effects models. Journal of Statistical Software. 82 (2017).

90. ^Liu T, et al. Developmental pattern of association fibers and their interaction with associated cortical microstructures in 0–5-month-old infants. NeuroImage. 261, 119525 (2022).

91. ^Gilles F, Shankle W, Dooling E. in Myelinated tracts: Growth patterns (eds Gilles F, Leviton A, Dooling E.) The Developing Human Brain 117–183 (Elsevier, 1983).

92. a, bDubois J, Adibpour P, Poupon C, Hertz-Pannier L, Dehaene-Lambertz G. MRI and M/EEG studies of the white matter development in human fetuses and infants: Review and opinion. Brain Plasticity 2, 49–69 (2016).

93. a, bLiu F, Feng J, Chen G, Shen D, Yap P-T. Gaussianization of diffusion mri data using spatially adaptive filtering. Medical Image Analysis 68, 101828 (2021).

94. a, bLiu F, et al. Does perfect filtering really guarantee perfect phase correction for diffusion mri data? Computerized Medical Imaging and Graphics 103, 102160 (2023).

95. a, bZhang F, et al. Quantitative mapping of the brain's structural connectivity using diffusion MRI tractography: A review. NeuroImage 249, 118870 (2022).

96. ^Seabold S, Perktold J. Not P (ed.) Statsmodels: Econometric and statistical modeling with python. (ed. Not P.) Proceedings of the 9th Python in Science Conference (SciPy, Vol. 7 (2010).

97. ^Sanchez-Alonso S, Aslin RN. Towards a model of language neurobiology in early development. Brain and Language 224, 105047 (2022).

98. a, bDai Y, Shi F, Wang L, Wu G, Shen D. iBEAT: A toolbox for infant brain magnetic resonance image processing. Neuroinformatics 11, 211–225 (2013).

99. a, b, c, d, e, fLiu F, et al. Not P (ed.) Harmonizing Multi-Modality Biases in Infant Development Analysis with an Integrated MRI Data Processing Pipeline. (ed.Not P.) Proceedings of ISMRM (2024).

100. ^Liu F, et al. Not P (ed.) NeoAudi Tract: An Automated Tool for Identifying Auditory Fiber Bundles in Infants. (ed.Not P.) Proceedings of ISMRM (2024).

101. a, b, cLiu J, et al. Greenspan H, et al. (eds) Adult-like phase and multi-scale assistance for isointense infant brain tissue segmentation. (eds Greenspan H, et al.) International Conference on Medical Image Computing and Computer-Assiste

d Intervention (MICCAI), 56–66 (Springer, 2023).

102. ^*Gu J, et al. Not P (ed.) Auditory fiber bundle parcellation using text-prompted decomposition networks. (ed.Not P.) IEEE 20th International Symposium on Biomedical Imaging (ISBI), 1–5 (2023).*

103. a, b, c, d*Chen L, et al. A 4D infant brain volumetric atlas based on the UNC/UMN baby connectome project (BCP) cohort. NeuroImage 253, 119097 (2022).*

104. a, b, c, d*Liu J, et al. Linguraru MG, et al. (eds) UinTSeg: Unified infant brain tissue segmentation with anatomy delineation. (eds Linguraru MG, et al.) International Conference on Medical Image Computing and Computer-Assisted Intervention (MICCAI), 54–65 (Springer, 2024).*

105. ^*Teng L, et al. Unified model for children's brain image segmentation with co-registration framework guided by longitudinal MRI. IEEE Journal of Biomedical and Health Informatics (2024).*

106. a, b*Liu J, et al. Structure-aware brain tissue segmentation for isointense infant MRI data using multi-phase multi-scale assistance network. IEEE Journal of Biomedical and Health Informatics (2024).*

107. a, b, c, d*Van Essen DC, et al. The WU-Minn human connectome project: An overview. NeuroImage 80, 62–79 (2013).*

108. ^*Moore JK, Linthicum Jr. FH. The human auditory system: A timeline of development. International Journal of Audiology 46, 460–478 (2007).*

109. ^*Galantucci B, Fowler CA, Turvey MT. The motor theory of speech perception reviewed. Psychonomic Bulletin & Review 13, 361–377 (2006).*

110. a, b*Hickok G, Poeppel D. The cortical organization of speech processing. Nature Reviews Neuroscience 8, 393–402 (2007).*

111. ^*Heyes C, Bird G. in Mirroring, association, and the correspondence problem 22 edn, (eds Haggard P, Rossetti Y, Kawato M.) Sensorimotor foundations of higher cognition 461–480 (Oxford University Press, 2007).*

112. ^*Heyes C, Catmur C. What happened to mirror neurons? Perspectives on Psychological Science 17, 153–168 (2022).*

113. ^*Catmur C, et al. Through the looking glass: Counter-mirror activation following incompatible sensorimotor learning. European Journal of Neuroscience 28, 1208–1215 (2008).*

114. ^*Meltzoff AN, Moore MK. Imitation of facial and manual gestures by human neonates. Science 198, 75–78 (1977).*

115. ^*Hayes LA, Watson JS. Neonatal imitation: Fact or artifact? Developmental Psychology 17, 655 (1981).*

116. ^*Field TM, Woodson R, Greenberg R, Cohen D. Discrimination and imitation of facial expression by neonates. Science 218, 179–181 (1982).*

117. ^*Koepke JE, Hamm M, Legerstee M, Russell M. Neonatal imitation: Two failures to replicate. Infant Behavior and Development 6, 97–102 (1983).*

118. ^*Anisfeld M, et al. No compelling evidence that newborns imitate oral gestures. Infancy 2, 111–122 (2001).*

119. ^*Oostenbroek J, et al. Comprehensive longitudinal study challenges the existence of neonatal imitation in humans. Current Biology 26, 1334–1338 (2016).*

120. ^*Meltzoff AN. Elements of a comprehensive theory of infant imitation. Behavioral and Brain Sciences 40 (2017).*

121. ∧*Meltzoff AN, et al. Re-examination of Oostenbroek, et al. (2016): Evidence for neonatal imitation of tongue protrusion. Developmental Science. 21: e12609 (2018).*

122. ∧*Oostenbroek J, et al. Re-evaluating the neonatal imitation hypothesis. Developmental Science. 22: e12720 (2018).*

123. ∧*Nagy E, Pilling K, Blake V, Orvos H. Positive evidence for neonatal imitation: A general response, adaptive engagement. Developmental Science. 23: e12894 (2020).*

124. ∧*Meltzoff AN, et al. Eliciting imitation in early infancy. Developmental Science. 22: e12738 (2018).*

125. ∧*Redshaw J. Re-analysis of data reveals no evidence for neonatal imitation in rhesus macaques. Biology Letters. 15: 20190342 (2019).*

126. ∧*Redshaw J, et al. Individual differences in neonatal "imitation" fail to predict early social cognitive behaviour. Developmental Science. 23: e12892 (2020).*

127. ∧*Davis J, et al. Does neonatal imitation exist? Insights from a meta-analysis of 336 effect sizes. Perspectives on Psychological Science. 16: 1373–1397 (2021).*

128. ∧*Fields RD. Change in the brain's white matter. Science. 330: 768–769 (2010).*

129. ∧*Lebel C, Deoni S. The development of brain white matter microstructure. NeuroImage. 182: 207–218 (2018).*

130. ∧*Kalyvas A, et al. Mapping the human middle longitudinal fasciculus through a focused anatomo-imaging study: Shifting the paradigm of its segmentation and connectivity pattern. Brain Structure and Function. 225: 85–119 (2020).*

131. ∧*Bristow D, et al. Hearing faces: How the infant brain matches the face it sees with the speech it hears. Journal of Cognitive Neuroscience. 21: 905–921 (2008).*

132. a, b*Jones SS. The development of imitation in infancy. Philosophical Transactions of the Royal Society B: Biological Sciences. 364: 2325–2335 (2009).*

133. ∧*Chen Y, et al. Simultaneous bilateral cochlear implantation in very young children improves adaptability and social skills: A prospective cohort study. Ear and Hearing. 44: 254–263 (2023).*

134. ∧*Friedmann N, Rusou D. Critical period for first language: The crucial role of language input during the first year of life. Current Opinion in Neurobiology. 35: 27–34 (2015).*

135. ∧*Joint Committee on Infant Hearing. Year 2019 position statement: Principles and guidelines for early hearing detection and intervention programs. Journal of Early Hearing Detection and Intervention. 4: 1–44 (2019).*

136. ∧*Houston DM, Miyamoto RT. Effects of early auditory experience on word learning and speech perception in deaf children with cochlear implants: Implications for sensitive periods of language development. Otology & Neurotology. 31: 1248–1253 (2010).*

137. ∧*Chang Y, Lee HR, Paik JS, Lee KY, Lee SH. Voxel-wise analysis of diffusion tensor imaging for clinical outcome of cochlear implantation: Retrospective study. Clinical and Experimental Otorhinolaryngology. 5: S37–S42 (2012).*

138. ∧*Huang L, et al. Diffusion tensor imaging of the auditory neural pathway for clinical outcome of cochlear implantation in pediatric congenital sensorineural hearing loss patients. PloS One. 10: e0140643 (2015).*

139. ∧*Tarabichi O, et al. Diffusion tensor imaging of central auditory pathways in patients with sensorineural hearing loss: A systematic review. Otolaryngology– Head and Neck Surgery. 158: 432–442 (2018).*

140. ∧*Spillmann L, et al. Gestalt neurons and emergent properties in visual perception: A novel concept for the transformatio n from local to global processing. Journal of Vision. 23: 4–4 (2023).*

141. a, b*Wasserthal J, Neher P, Maier-Hein KH. TractSeg-Fast and accurate white matter tract segmentation. NeuroImage. 1 83: 239–253 (2018).*

142. ∧*Glasser MF, et al. The minimal preprocessing pipelines for the Human Connectome Project. NeuroImage. 80: 105–124 (2013).*

143. ∧*Avants B, Gee JC. Geodesic estimation for large deformation anatomical shape averaging and interpolation. NeuroIma ge. 23: S139–S150 (2004).*

144. ∧*Avants BB, Tustison N, Song G, et al. Advanced normalization tools (ANTs). Insight J. 2: 1–35 (2009).*

145. ∧*Avants BB, et al. A reproducible evaluation of ANTs similarity metric performance in brain image registration. NeuroI mage. 54: 2033–2044 (2011).*

146. ∧*Dhollander T, Raffelt D, Connelly A. Not, P. (ed.) Unsupervised 3-tissue response function estimation from single-shell or multi-shell diffusion MR data without a co-registered T1 image. (ed.Not, P.) ISMRM workshop on breaking the barri ers of diffusion MRI, Vol. 5 (Lisbon, Portugal, 2016).*

147. ∧*Tournier JD, Calamante F, Connelly A. Robust determination of the fibre orientation distribution in diffusion MRI: Non -negativity constrained superresolved spherical deconvolution. NeuroImage. 35: 1459–1472 (2007).*

148. a, b, c*Tournier JD, et al. MRtrix3: A fast, flexible and open software framework for medical image processing and visuali sation. NeuroImage. 202: 116137 (2019).*

149. ∧*Avants BB, Epstein CL, Grossman M, Gee JC. Symmetric diffeomorphic image registration with cross-correlation: eval uating automated labeling of elderly and neurodegenerative brain. Medical Image Analysis. 12: 26–41 (2008).*

150. ∧*Klein A, Tourville J. 101 labeled brain images and a consistent human cortical labeling protocol. Frontiers in Neuroscie nce. 6: 1–12 (2012).*

151. ∧*Xiao B, Suk HI, Liu M, Yan P, Lian C, editors. Weakly supervised confidence learning for brain mr image dense parcella tion. In: Suk HI, Liu M, Yan P, Lian C, editors. Proceedings of International Workshop on Machine Learning in Medical I maging (MLMI). Springer; 2019. p. 409–416.*

152. ∧*Jenkinson M, Beckmann CF, Behrens TE, Woolrich MW, Smith SM. FSL. NeuroImage. 2012;62:782–790.*

153. a, b*Tustison NJ, et al. N4ITK: Improved N3 bias correction. IEEE TMI. 2010;29:1310–1320.*

154. ∧*Wang L, et al. iBEAT V2.0: A multisite-applicable, deep learning-based pipeline for infant cerebral cortical surface rec onstruction. Nature Protocols. 2023;18:1488–1509.*

155. ∧*Garyfallidis E, et al. Quickbundles, a method for tractography simplification. Frontiers in Neuroscience. 2012;6:175.*

156. ∧*Andersson JL, Skare S, Ashburner J. How to correct susceptibility distortions in spin-echo echo-planar images: Applica tion to diffusion tensor imaging. NeuroImage. 2003;20:870–888.*

157. ∧*Andersson JL, Graham MS, Zsoldos E, Sotiropoulos SN. Incorporating outlier detection and replacement into a non-pa rametric framework for movement and distortion correction of diffusion MR images. NeuroImage. 2016;141:556–572.*

158. ^*Kellner E, Dhital B, Kiselev VG, Reisert M. Gibbs-ringing artifact removal based on local subvoxel-shifts. Magnetic Resonance in Medicine. 2016;76:1574–1581.*

159. ^*Raffelt D, et al. Not P, editor. Bias field correction and intensity normalisation for quantitative analysis of apparent fibre density. In: Not P, editor. Proceedings of ISMRM. 2017;25:3541.*

160. ^*Cordero-Grande L, Christiaens D, Hutter J, Price AN, Hajnal JV. Complex diffusion-weighted image estimation via matrix recovery under general noise models. NeuroImage. 2019;200:391–404.*

161. ^*Jenkinson M, Smith S. A global optimisation method for robust affine registration of brain images. Medical Image Analysis. 2001;5:143–156.*

162. ^*Greve DN, Fischl B. Accurate and robust brain image alignment using boundary-based registration. NeuroImage. 2009;48:63–72.*

163. ^*Andersson JL, Sotiropoulos SN. An integrated approach to correction for off-resonance effects and subject movement in diffusion MR imaging. NeuroImage. 2016;125:1063–1078.*

164. ^*Dhollander T, et al. Not P, editor. Multi-tissue log-domain intensity and inhomogeneity normalisation for quantitative apparent fibre density. In: Not P, editor. Proceedings of ISMRM. 2021;29:2472.*

165. ^*Tournier JD, Calamante F, Connelly A, et al. Not P, editor. Improved probabilistic streamlines tractography by 2nd order integration over fibre orientation distributions. In: Not P, editor. Proceedings of ISMRM. 2010;1670.*

166. ^*Holdsworth SJ, et al. Diffusion tensor imaging (DTI) with retrospective motion correction for large-scale pediatric imaging. Journal of Magnetic Resonance Imaging. 2012;36:961–971.*

Declarations

Potential competing interests: No potential competing interests to declare.